




Neuron-restrictive silencer factor/repressor element 1-silencing transcription factor (NRSF/REST) controls spatial K⁺ buffering in primary cortical astrocytes

Eleonora Centonze^{1,2}  | Antonella Marte^{2,3}  | Martina Albini^{1,2}  | Anna Rocchi^{1,3}  |
Fabrizia Cesca^{1,4}  | Martina Chiacchiaretta¹  | Thomas Floss⁵  | Pietro Baldelli^{2,3}  |
Stefano Ferroni⁶  | Fabio Benfenati^{1,3}  | Pierluigi Valente^{2,3} 

¹Center for Synaptic Neuroscience and Technology, Istituto Italiano di Tecnologia, Genova, Italy

²Department of Experimental Medicine, Section of Physiology, University of Genova, Genova, Italy

³IRCSS Ospedale Policlinico San Martino, Genova, Italy

⁴Department of Life Sciences, University of Trieste, Trieste, Italy

⁵Helmholtz Zentrum München, Deutsches Forschungszentrum für Gesundheit und Umwelt (GmbH), Neuherberg, Germany

⁶Department of Pharmacy and Biotechnology, University of Bologna, Bologna, Italy

Correspondence

Fabio Benfenati and Pierluigi Valente, IRCSS, Ospedale Policlinico San Martino, 16132 Genova, Italy.

Email: fabio.benfenati@iit.it and pierluigi.valente@unige.it

Present address

Eleonora Centonze, Department of Biomedical Sciences, University of Lausanne, Lausanne, Switzerland

Martina Chiacchiaretta, Department of Neuroscience, Tuft University School of Medicine, Boston, Massachusetts, USA

Abstract

Neuron-restrictive silencer factor/repressor element 1 (RE1)-silencing transcription factor (NRSF/REST) is a transcriptional repressor of a large cluster of neural genes containing RE1 motifs in their promoter region. NRSF/REST is ubiquitously expressed in non-neuronal cells, including astrocytes, while it is down-regulated during neuronal differentiation. While neuronal NRSF/REST homeostatically regulates intrinsic excitability and synaptic transmission, the role of the high NRSF/REST expression levels in the homeostatic functions of astrocytes is poorly understood. Here, we investigated the functional consequences of NRSF/REST deletion in primary cortical astrocytes derived from NRSF/REST conditional knockout mice (KO). We found that NRSF/REST KO astrocyte displayed a markedly reduced activity of inward rectifying K⁺ channels

Abbreviations: AMPA, α -amino-3-hydroxy-5-methyl-4-isoxazolepropionic acid; AP, action potential; BSA, bovine serum albumin; CNQX, 6-Cyano-7-nitroquinoxaline-2,3-dione; D-AP5, D-(-)-2-amino-5-phosphonopentanoic acid; DIV, days in vitro; DMEM, Dulbecco's modified eagle medium; E18, 18-day mouse embryos; EAAT1, excitatory amino acid transporters 1; EAAT2, excitatory amino acid transporters 2; ECL, enhanced chemiluminescence; EDTA, ethylene diamine tetraacetic acid; E_{rev} , reversal potential; FBS, fetal bovine serum; GABA, γ -aminobutyric acid; GFP, green fluorescent protein; GLAST, glutamate/aspartate transporter; GLT-1, glutamate transporter-1; ³H-Glu, 3H-labeled glutamate; H3K9, Histone H3 lysine 9; IL-1 β , interleukin-1 β ; K⁺ ext, extracellular K⁺; K_{2p}, two-pore domains K⁺ channels; Kir, K⁺ inward rectifier; KO, knockout; MeCP2, methyl-CpG binding protein 2; mEPSC, miniature excitatory postsynaptic current; MOI, multiplicity of infection; NMDA, N-methyl-D-aspartate; NRSF, Neuron-restrictive silencer factor; PBS, phosphate buffered saline; RE1, repressor element 1; REST, repressor element 1-silencing transcription factor; R_{input}, input resistance; RRID, Research Resource Identifier (see scicrunch.org); RT, room temperature; SEM, standard error of the mean; SDS-PAGE, sodium dodecyl sulphate–polyacrylamide gel electrophoresis; TBOA, three- β -benzyloxyaspartic acid; TTX, tetrodotoxin; UCPH, 2-amino-5,6,7,8-tetrahydro-4-(4-methoxyphenyl)-7-(naphthalen-1-yl)-5-oxo-4H-chromene-3 carbonitrile; V_h, holding potential; V_{rest}, resting membrane potential.

Eleonora Centonze, Antonella Marte are co-first authors, Fabio Benfenati and Pierluigi Valente are co-last authors and equally contributed to this work.

subtype 4.1 (Kir4.1) underlying spatial K⁺ buffering that was associated with a decreased expression and activity of the glutamate transporter-1 (GLT-1) responsible for glutamate uptake by astrocytes. The effects of the impaired astrocyte homeostatic functions on neuronal activity were investigated by co-culturing wild-type hippocampal neurons with NRSF/REST KO astrocytes. Interestingly, neurons experienced increased neuronal excitability at high firing rates associated with decrease after hyperpolarization and increased amplitude of excitatory postsynaptic currents. The data indicate that astrocytic NRSF/REST directly participates in neural circuit homeostasis by regulating intrinsic excitability and excitatory transmission and that dysfunctions of NRSF/REST expression in astrocytes may contribute to the pathogenesis of neurological disorders.

KEYWORDS

glutamate uptake, NRSF/REST, potassium channels, primary astrocytes, synaptic homeostasis, transcriptional regulation

1 | INTRODUCTION

Neuron-restrictive silencer factor/repressor element 1 (RE1)-silencing transcription factor (NRSF/REST, henceforth referred to as REST) is a master transcriptional regulator that modulates diverse sets of protein-coding and non-coding genes (Baldelli & Meldolesi, 2015; Chong et al., 1995; Schoenherr & Anderson, 1995). REST binds to gene promoters containing one or more RE1 consensus sites and mediates cell-specific gene repression by recruiting the co-repressors mSin3a and CoREST at its N- and C-terminal domains respectively. Co-repressors, in turn, recruit multiple chromatin-remodeling factors, including the methyl DNA-binding protein MeCP2 and the histone deacetylase and histone H3K9 methyltransferase G9a, which produce chromatin remodeling and nucleosome repositioning (Ballas et al., 2005; Ballas & Mandel, 2005; Zheng et al., 2009), ultimately repressing gene transcription (Abrajano et al., 2009a; Grimes et al., 2000; Schoenherr & Anderson, 1995). Many of the over 2000 REST-controlled genes are neuron-specific, including those encoding neurotransmitter synthesizing enzymes, synaptic vesicle and cytoskeletal proteins, growth factors and adhesion molecules, ion channels and neurotransmitter receptors (Bruce et al., 2004; Schoenherr et al., 1996; Schoenherr & Anderson, 1995).

In recent years, a growing body of experimental evidence has demonstrated that, in the developing brain, REST sets the appropriate proportion of neuronal and astrocytic cells and controls their differentiation (Abrajano et al., 2009b; Covey et al., 2012; Dewald et al., 2011). In neurons, REST expression is sensitive to the levels of physiological activity and mediates homeostatic plasticity responses to hyperexcitability at the level of both intrinsic excitability and synaptic transmission (Pecoraro Bisogni et al., 2018; Pozzi et al., 2013; Prestigio et al., 2021). High REST levels are also crucial for directing the differentiation of astrocytes to specific phenotypes (Kohyama et al., 2010).

Astrocytes are the most abundant neuroglial cell type of the brain known for their high morphological and functional heterogeneity. They have a central role in physiological brain signaling and their dysfunction is critical in the pathogenesis of several disorders (for review see, Verkhatsky & Nedergaard, 2018; Aronica et al., 2012). They take part in the so-called “tripartite synapse”, where an intimate relationship between the pre/postsynaptic neural components and perisynaptic astrocytes occurs (Araque et al., 1999; Quesseveur et al., 2013). At the synapse, astrocytes sense neural activity, maintain the homeostasis of the extracellular environment and participate in information processing within neuronal networks by controlling neuronal excitability (Walz, 2000).

During neuronal activity, the large amounts of K⁺ and glutamate that are released extracellularly must be correctly buffered, to prevent network hyperactivity. The inwardly rectifying K⁺ (Kir) channel containing the subunit Kir4.1, specifically expressed in astrocytic processes surrounding synapses, but not in neurons (Higashi et al., 2001), has been identified as a principal mediator for spatial K⁺ buffering in the astroglial syncytium (Olsen & Sontheimer, 2008). Of note, variations in functional expression of astroglial Kir4.1 have been shown in several neurodevelopmental and genetic disorders as well as in neurodegenerative diseases (Nwaobi et al., 2016), that are conditions in which alterations of REST activity are also observed (Garcia-Manteiga et al., 2020; Zhao et al., 2017).

The Kir4.1 channel is also responsible for establishing and maintaining the astrocytic resting membrane potential and its activity is directly linked to glutamate uptake by astrocytes (Olsen & Sontheimer, 2008). Astrocytes express two glutamate transporters, namely excitatory amino acid transporter 1 (EAAT2 or GLT-1) and the glutamate-aspartate transporter (EAAT1 or GLAST) (Dallérac et al., 2018; Lee et al., 2009). The activity of GLT-1, the more abundant astrocyte glutamate transporter, is strictly related to the maintenance of a hyperpolarized membrane potential by Kir4.1 to ensure maximal rates of glutamate transport. It has been observed that

down-regulation of Kir4.1 or its functional block by Ba²⁺ is followed by a reduction of glutamate uptake by GLT-1 (Kucheryavykh et al., 2007). In addition, Kir4.1 conditional knockout (KO) mice are characterized by impaired K⁺ buffering and glutamate uptake, hyperexcitability and seizures (Chever et al., 2010; Djukic et al., 2007). A similar phenotype is observed in mice bearing a primary down-regulation of GLT-1 (Rothstein et al., 1994, 1996). The strict functional link between Kir4.1 and GLT-1 suggests that the two membrane actuators form a supra-molecular complex on the membrane of astrocytes.

In this paper, we analyzed the impact of *Rest* deletion on the function of primary cortical astrocytes derived from a complete *Rest* conditional KO mice (Nechiporuk et al., 2016). We observed that *Rest* deletion caused a significant depolarization of the resting membrane potential by reducing Kir4.1-mediated K⁺ currents. This effect was caused by a decreased density of Kir4.1 exposed at the plasma membrane and was associated with a decreased glutamate uptake by GLT-1, an effect consistent with the positive modulation of GLT-1 expression by REST recently shown to protect dopamine neurons from Mn-induced neurotoxicity (Pajarillo et al., 2021, 2022). In addition, wild-type neurons co-cultured with *Rest*-KO astrocytes showed decrease afterhyperpolarization, increased excitability at high firing rates and increased strength of glutamatergic transmission. The study demonstrates a role of REST-directed epigenetic processes in the maintenance of the homeostatic functions of astrocytes, such as K⁺-buffering and glutamate uptake, and implicates astrocytes in the pathogenesis of neurological diseases associated with *Rest* dysregulation.

2 | MATERIALS AND METHODS

2.1 | Experimental animals

Wild-type C57BL/6J mice were obtained from Charles River (Calco, Italy). Heterozygous GTinvREST mice (REST^{GTi} mice; Nechiporuk et al., 2016) were kindly provided by Gail Mandel (Portland, United States) and the German Gene Trap Consortium (GGTC-Partners). Animals were maintained on a C57BL/6J background and kept in homozygosity. Two females were housed with one male in standard Plexiglas cages (33×13 cm), with sawdust bedding and metal top. After 2 days of mating, male mice were withdrawn, and dams were housed individually in plexiglass cages and checked daily. Mice were weaned into cages of same sex pairs. Mice were maintained on a 12:12h light/dark cycle (lights on at 7 a.m.) at constant temperature (22±1°C) and relative humidity (60±10%), provided drinking water and a complete pellet diet (Mucedola, Settimo Milanese, Italy) ad libitum, and housed under conditions of environmental enrichment in the IRCCS Ospedale Policlinico San Martino Animal Facility. All efforts were made to minimize suffering and reduce the number of animals used. All experiments were carried out in accordance with the guidelines established by the European Community Council (Directive 2010/63/EU of 22 September 2010) and approved by the Italian Ministry of Health (Authorizations #73-2014-PR and

#558/2016-PR). For the experiments, we have used 15 and 5 animals for astrocytic and neuronal preparations respectively. For primary cultures of astrocytes about six pups were used for dissection. For primary cultures of hippocampal neurons, 6–8 embryos were used for dissection. The flowchart of the experimental plan, whose details are listed below, is shown in Figure S1.

2.2 | Primary astrocyte cultures

Primary postnatal cortical astrocytic cultures were prepared from homozygous REST^{GTi} mice (Nechiporuk et al., 2016) as previously described (Chiacchiaretta et al., 2018; Ferroni et al., 2003). Newborn pups (P0 to P2) were killed under deep carbon dioxide anesthesia. Brains were pooled during primary cell preparation. After removal of the meninges, cortical tissue was enzymatically dissociated. Astrocytes were plated on poly-D-lysine-coated (0.01mg/mL) cell culture flasks and incubated for about 2 weeks at 37°C, 5% CO₂, 90% humidity in a medium consisting of DMEM (Gibco/Thermo-Fischer Scientific) supplemented to reach the final concentration of 1% glutamine, 1% penicillin/streptomycin, and 10% Fetal Bovine Serum (FBS; Gibco/Thermo-Fischer Scientific). At confluence, astrocytes were enzymatically detached with trypsin-EDTA and plated on 33-mm Petri dishes at a density of 40000 or 100000 cells/mL, depending on the experiment.

2.3 | Preparation of viral vectors and transduction of primary astrocytes

Sequences containing active or inactive Cre-recombinase were cloned into lentiviral vectors under the control of the constitutive phosphoglycerokinase (PGK) promoter, generating pLenti-PGK-Cre-EGFP or pLenti-PGK-ΔCre-EGFP plasmids respectively (Jaudon et al., 2020; Kaeser et al., 2011). The production of VSV-pseudotyped third-generation lentiviruses was performed as previously described (De Palma & Naldini, 2002; Rocchi et al., 2021). The transduction of primary astrocytes obtained from homozygous Rest^{GTi} mouse cortices, with lentiviruses expressing Cre, but not ΔCre, results in re-inversion of the GTinv cassette, terminating transcription upstream of remaining REST sequences. The same cultures of primary astrocytes were transduced with lentivirus encoding either Cre or ΔCre 3 days after plating at a multiplicity of infection of 10 (MOI). After 24 h of infection, half of the medium was replaced with fresh medium. All experiments were performed 7 days after transduction. Transduction efficiency was always above 75% of astrocytes, as verified by evaluating the nuclear expression of the GFP reporter.

2.4 | Astrocyte/neuron co-cultures

For the astrocyte/neuron co-culture experiments, astrocytes were seeded on poly-D-lysine-coated (0.01mg/mL) on Petri dishes

(33-mm diameter) at a density of 200000 cells/mL. After 3 days of incubation, astrocytes were subjected to infection with lentivirus containing Δ Cre and Cre enzymes and the medium was replaced after 24 h. Six days later, the complete DMEM medium was replaced with Neurobasal (Gibco/Thermo-Fischer Scientific) supplemented to reach the final concentration of 10% FBS, 1% glutamine, 1% penicillin/streptomycin, and 2% B27 (Gibco/Thermo-Fischer Scientific). The day after, enzymatically dissociated hippocampal neurons obtained from 18-day mouse embryos (E18) were plated on the top of astrocytes at a density of 200000 cells/mL in complete Neurobasal medium, as described above. Two hours later, all medium was replaced with Neurobasal supplemented with 1% glutamine, 1% penicillin/streptomycin, and 2% B27.

2.5 | Surface biotinylation and immunoblotting

Seven days after infection, cultured cortical astrocytes were washed three times with cold phosphate buffered saline (PBS). Astrocytes were incubated with 1 mg/mL biotin (EZLink Sulfo-NHS-LC-Biotin, Thermo Fisher Scientific, #21335) in PBS pH 8 for 30 min at 4°C. After biotin withdrawal, astrocytes were washed twice with Tris 50 mM pH 8, followed by two washes with PBS pH 8.

Astrocytes were lysed with lysis buffer (150 mM NaCl, 50 mM TrisCl, pH 7.4, 1 mM EDTA, 1% Triton X-100) supplemented with protease inhibitors. After 10 min of incubation on ice, cell lysates were collected and clarified by centrifugation (10 min at 10000 \times g at 4°C). Supernatants were incubated with NeutrAvidin agarose resin (Thermo Fisher Scientific, #29202) at 4°C for 3 h. Proteins were eluted from the agarose resin, resolved by SDS/PAGE and revealed by immunoblotting using the ECL chemiluminescence detection system (ThermoFisher Scientific). The following antibodies were used: mouse monoclonal anti-inwardly rectifying potassium channel containing the 4.1 subunit (Kir4.1; Santa Cruz, sc-293252), rabbit polyclonal anti-GLT-1 (EAAT2, Cell Signaling Technology, #3838; [RRID:AB_2190743](#)), mouse monoclonal anti-actin (Sigma-Aldrich Cat# A4700, [RRID:AB_476730](#)), rabbit monoclonal anti-GAPDH (Cell Signaling Technology Cat# 2118, [RRID:AB_561053](#)), mouse monoclonal anti-Na⁺/K⁺ ATPase alpha-1 (Millipore Cat# 05-369, [RRID:AB_309699](#)), guinea pig polyclonal anti-GLAST (Chemicon/Millipore Cat# AB1782). Chemiluminescence intensity was quantified using the ChemiDoc MP Imaging System (GE Healthcare BioSciences, Buckinghamshire, UK). To test GLT-1 turnover, astrocytes were treated with cycloheximide (Chx, 50 μ g/mL; #C1988, Sigma Aldrich) for 16 h.

2.6 | Immunofluorescence

Seven days after infection, cultured cortical astrocytes were fixed in PBS with 4% paraformaldehyde (PFA) for 15 min at room

temperature (RT) and then washed with PBS. Cells were permeabilized with 0.1% Triton X-100 in PBS for 5 min at RT and blocked with 2% bovine serum albumin (BSA) in PBS for 30 min. Cells were incubated with primary antibodies in PBS 2% BSA overnight at 4 °C. Astrocytes were immunostained with monoclonal antibodies to glial fibrillary acidic protein (GFAP, Sigma Aldrich, Milan, Italy #G3893, [RRID:AB_477010](#)). After several PBS washes, astrocytes were incubated with the fluorescent secondary antibodies in the blocking buffer solution for 1 h. After washing in PBS for three times, astrocytes were stained with Hoechst for nuclear detection. After several washes in PBS, coverslips were mounted with Mowiol mounting medium. All images used for quantification of the immunofluorescence intensity were acquired with a Leica SP8 confocal microscopy (Leica Microsystems, Wetzlar, Germany). Images were obtained using a 63x oil objective at a resolution of 1024 \times 1024 pixels and Z-stacks were acquired every 300 nm. For each set of experiments, all images were acquired using identical exposure settings. Offline analysis was performed using the ImageJ software. Astrocyte morphology was quantified by using the “Polygon Selections” feature tool and the “Measure” function of ImageJ yielding the following shape descriptors: field area (μ m²), field perimeter (μ m), and circularity index. The circularity function calculates object circularity using the formula: circularity = $4\pi(\text{area}/\text{perimeter}^2)$, ranging from 0 (infinitely elongated polygon) to 1.0 (perfect circle).

2.7 | ³H-glutamate uptake assay

For glutamate uptake experiments, astrocytes were plated at concentration of 2×10^5 cells/mL in 6-well plates and the experiments were performed as previously described (Chiacchiaretta et al., 2018). Briefly, astrocyte cultures were washed three times with pre-warmed (37°C) HEPES-buffered Hanks-balanced salt solution. One μ Ci/mL of L-[3,4-³H]-glutamate (NET490001MC, Perkin Elmer, Milan, Italy) was added to unlabeled L-glutamate (#G8415, Sigma) at a final concentration of 50 μ M in standard extracellular solution containing (in mM): 140 NaCl, 4 KCl, 2 MgCl₂, 2 CaCl₂, 10 HEPES, 5 D-glucose. To isolate GLT-1 operated glutamate transport, the GLAST specific inhibitor 40-amino-5,6,7,8-tetrahydro-4-(4-methoxyphenyl)-7-(naphthalen-1-yl)-5-oxo-4Hchromene-3-carbonitrile (UCPH) was added throughout (10 μ M). To detect the Na⁺-independent transport, NaCl was replaced by choline chloride (#C7017, Sigma). To isolate Kir4.1-mediated glutamate uptake, a saturating concentration of Ba²⁺ (600 μ M; #342920, Sigma) was added to the extracellular solution. To block glutamate transporters, TBOA (100 μ M; #2532, Tocris) was added. Cultures were incubated with the isotope on a heating plate at 37°C for 10 min. After three washes with PBS, cells were harvested into 400 μ L of 1 M NaOH solution in MilliQ water. Samples were transferred to vials containing 2 mL of aqueous scintillation mixture and counted using a liquid scintillation counter (1450 LSC & Luminescence Counter, MicroBete TriLux, Perkin Elmer).

2.8 | Patch-clamp recordings

2.8.1 | Primary astrocytes

Infected astrocytes of both phenotypes were used for patch-clamp electrophysiological recordings using the whole-cell configuration as previously described (Ferroni et al., 1995). The experiments were performed 7 days *in vitro* (DIV) after infection, using an EPC-10 amplifier controlled by PatchMaster software (HEKA Elektronik, Lambrecht/Pfalz, Germany) and an inverted DMI6000 microscope (Leica Microsystems GmbH, Wetzlar, Germany). Patch electrodes fabricated from thick borosilicate glasses were pulled to a final resistance of 4–5 M Ω when filled with the standard internal solution. Recordings with leak current >200 pA or series resistance >10 M Ω were discarded. All recordings were acquired at 50 kHz. Experiments were carried out at RT (20–24°C). Salts and other chemicals were of the highest purity grade (Sigma, St. Louis, MO). For the experiments involving astrocytes, the standard bath saline contained (mM): 140 NaCl, 4 KCl, 2 MgCl₂, 2 CaCl₂, 10 HEPES, 5 glucose, pH 7.4, with NaOH and osmolarity adjusted to ~315 mOsm/L with mannitol. The intracellular (pipette) solution was composed of (mM): 144 KCl, 2 MgCl₂, 5 EGTA, 10 HEPES, pH 7.2 with KOH and osmolarity ~300 mOsm/L. Experiments carried out under various extracellular K⁺ concentrations (K⁺_{ext}) were done using external solutions with K⁺ salts replaced equimolarly. Aliquots of BaCl₂ were prepared in MilliQ and 0.2 mM of Ba²⁺ were added to the extracellular solution to block K⁺ channels, in the presence of the internal solution described above. The different saline containing the pharmacologic agents was applied with a gravity-driven, local perfusion system at a flow rate of ~200 μ L/min positioned within ~100 μ m of the recorded astrocytes. The experiments with IL-1 β were performed by incubating astrocytes with IL-1 β (10 ng/mL) or a corresponding amount of vehicle (water) and patch-clamp experiments were done 24 h after incubation. In the experiments conducted with L-glutamate, external solutions with L-glutamate, previously aliquoted into extracellular solution, were used. One mM L-glutamate was added to the extracellular solution to stimulate GLT-1 transporters. To isolate the currents generated by GLT-1, 10 μ M of UCPH were added to the solution to selectively block GLAST. To block glutamate transporters, 100 μ M TBOA (#2532, Tocris) was used.

2.8.2 | Astrocyte/neuron co-cultures

For the experiment involving astrocyte/neuron co-cultures, cells were maintained in standard Tyrode solution containing (in mM): 140 NaCl, 4 KCl, 2 CaCl₂, 1 MgCl₂, 10 HEPES, 10 glucose, pH 7.3 with NaOH and osmolarity ~315 mOsm/L. For the analysis of neuronal excitability, D-(-)-2-amino-5-phosphonopentanoic acid (D-AP5; 50 μ M), 6-cyano-7-nitroquinoxaline-2,3-dione (CNQX; 10 μ M), and bicuculline methiodide (30 μ M), were added to block NMDA, non-NMDA, and GABA_A receptors respectively. The standard internal solution was (in mM): 126 K Gluconate, 4 NaCl, 1 MgSO₄, 0.02

CaCl₂, 0.1 BAPTA, 15 glucose, 5 HEPES, 3 ATP, 0.1 GTP (pH 7.2 with KOH). Current-clamp recordings of neuronal firing activity and the following analysis were performed as previously described (Valente et al., 2016). Neuronal cells were held at a potential of -70 mV and action potentials (APs) were induced by injection of 10 pA current steps of 1 s in pyramidal neurons morphologically identified by their teardrop-shaped somata and characteristic apical dendrite after 12–16 DIV (Prestigio et al., 2019; Watt et al., 2000). The mean firing frequency was calculated as the number of APs evoked by minimal current injection, whereas the instantaneous frequency was estimated as the reciprocal value of the time difference between the first two evoked APs. The rheobase was calculated as the minimum depolarizing current needed to elicit at least one AP. Current-clamp recordings were acquired at a 50 kHz and filtered at 1/5 of the acquisition rate with a low-pass Bessel filter. Miniature excitatory postsynaptic currents (mEPSCs) were recorded from low-density hippocampal neurons in standard external solution containing TTX (1 μ M; Tocris Bioscience), D-AP5 (50 μ M), bicuculline (30 μ M), and CGP 58845 (10 μ M) to block Na⁺ channels, NMDA, GABA_A and GABA_B receptors and generation and propagation of spontaneous action potentials (APs). The amplitude and frequency of mEPSCs were calculated using a peak detector function with appropriate threshold amplitude and threshold area using the Minianalysis program (Synaptosoft).

2.9 | Statistical analysis

The number of mice necessary for the project was preliminarily calculated based on the experimental variability and need to reach an appropriate number of replications for a robust statistical analysis and occasional loss of animals because of anesthesia or unpredictable factors. The number of animals determine for the planned experiments (sample size, n) was predetermined using the following formula: $n = Z^2 \times \sigma^2 / \Delta^2$, where: Z is the value of the distribution function $f(\alpha, \beta)$ (with α and β type-I and type-II errors, respectively; based on $\alpha = 0.05$ and $1 - \beta = 0.9$), σ is the standard deviation of the groups (set between 0.2–0.3 based on similar experiments and preliminary data) and Δ the minimum percent difference that is thought to be biologically relevant (0.2 or 20%). No randomization method was used, and no animals were excluded, as the study was entirely conducted *in vitro*. Experiments were carried out blind to the experimenter. No exclusion criteria were pre-determined. Data are expressed as means \pm standard error of the mean (sem) for number of cells (n) or mouse preparations as detailed in the figure legends. Normal distribution of data was assessed using the D'Agostino-Pearson's normality test. The F-test was used to compare variance between two sample groups. To compare two normally distributed sample groups, the Student's unpaired or paired 2-tailed t-test was used. To compare two sample groups that were not normally distributed, the nonparametric Mann-Whitney's U-test was used. To compare more than two normally distributed sample groups, we used one- or two-way ANOVA, followed by the Bonferroni's test. In cases

in which data were not normally distributed, one- and two-way ANOVA were substituted with the Kruskal–Wallis's and Friedman's two-way ANOVA tests, respectively, followed by the Dunn's multiple comparison test. The Grubbs's test was used to detect outliers at the 95% confidence level. Alpha levels for all tests were 0.05% (95% confidence intervals). Statistical analysis was carried out using OriginPro-8 (OriginLab Corp., Northampton, MA, USA) and Prism (GraphPad Software, Inc.) software.

3 | RESULTS

3.1 | *Rest*-deleted astrocytes preserve a normal cellular morphology

To explore the role of *Rest* in astrocyte differentiation and function, we used a conditional mouse model ($REST^{GTi}$) bearing a loxed inverted gene trap cassette between non-coding exon 1a–c and the first coding exon, exon 2 (Nechiporuk et al., 2016). *REST* gene expression in primary $REST^{GTi}$ astrocytes was knocked out by transduction with Cre recombinase (Figure 1a). Primary cortical astrocytes, obtained from the cortices of newborn homozygous $REST^{GTi}$ mice, were infected at 18 DIV with lentiviruses encoding either functional Cre recombinase (herein referred to as KO) or an inactive deletion mutant of Cre recombinase (Δ Cre) used as a control (Ctrl), together with nuclear green fluorescent protein (GFP) as a transduction reporter (Figure 1b). Infected astrocytes, cultured until 25–28 DIV, were examined morphologically, biochemically, and electrophysiologically. The transduction efficiency (~75–80%) was similar in both experimental groups and Cre-infected astrocytes showed a very low level of *Rest* mRNA and protein compared to astrocytes infected with Δ Cre (Figure 1c–e). Since evidence exists that the activity of *REST* influences the differentiation of primary astrocytes (Kohyama et al., 2010; Liu et al., 2019), and GFAP expression is related to astrocyte maturation, we evaluated the effect of *REST* deletion on GFAP expression and cellular distribution by measuring the GFAP immunoreactive area and circularity index. However, no detectable changes in these parameters were observed in Cre- (*Rest*-KO) and Δ Cre- (control) transduced astrocytes (Figure 1f).

3.2 | *Rest* deletion impairs the expression of the GLT1-transporter and glutamate uptake

Astrocytes express high levels of the Na^+ -dependent excitatory amino acid transporters GLT-1, responsible for 90% of the clearance of glutamate released into the synaptic cleft (Danbolt, 2001). The glutamate transport activity of GLT-1 known to be closely associated with Kir4.1 channels which set V_{rest} near the K^+ reversal potential and provide a large shunt conductance that limits the spread of transport-associated currents (Kucheryavykh et al., 2007; Tzingounis & Wadiche, 2007).

As *REST* is known to regulate brain homeostasis under physiological conditions, and canonical RE1 elements are present in the regulatory regions of the *Slc1A2* gene encoding for GLT-1, we first investigated whether *REST* deletion was affecting the expression and function of this major astrocyte glutamate transporter.

We found that *Rest* deletion was associated with a significant decrease of both GLT-1 mRNA (Figure 2a, left) and total protein levels (Figure 2b,c). Notably, when the multiplicity of infection for astrocyte transduction was varied, a significant correlation was found between the extent of *Rest* knockdown and the mRNA levels of GLT-1, indicating that the control of GLT-1 expression by *Rest* occurs at the transcriptional level (Figure 2a, right). No significant change in GLT-1 protein turnover was observed between control and *Rest*-KO astrocytes after protein synthesis inhibition with cycloheximide (Figure 2d). We also investigated how the decreased GLT-1 expression in *Rest* KO astrocytes was affecting the subcellular fate of GLT-1 between intracellular and membrane exposed compartments astrocytes by surface biotinylation experiments. The results show that the decrease in the total expression of GLT-1 in the absence of *Rest* was entirely reflected by a marked decrease of the fraction of the transporter targeted to the plasma membrane, while its intracellular pool was not affected (Figure 2b,c). We also investigated by immunoblotting whether the other glutamate transporter GLAST was affected by *Rest* deletion or was undergoing any increase to compensate for GLT-1 down-regulation. However, the protein levels of GLAST were not significantly affected by *Rest* deletion (Figure 2e).

3.3 | *Rest* deletion impairs glutamate uptake by the GLT1-transporter

Next, we analyzed whether the decreased expression and membrane targeting of GLT-1 in *Rest* KO astrocytes was translating into an impairment of glutamate uptake. To this aim, we assessed the 3H -labeled glutamate (3H -Glu) dynamics in control and *Rest*-KO astrocytes. The Na^+ -dependent component of glutamate uptake was isolated by replacing extracellular Na^+ with choline, the contribution of Kir4.1 channels to glutamate transport was challenged using Ba^{2+} and the GLT-1 operated transport upon administration of the specific GLT-1 inhibitor DL-threo- β -benzyloxyaspartic acid (TBOA, 100 μ M). To isolate the activity of GLT-1, all the experiments were carried out in the presence of 2-amino-5,6,7,8-tetrahydro-4-(4-met hoxyphenyl)-7-(naphthalen-1-yl)-5-oxo-4H-chromene-3 carbonitrile (UCPH, 10 μ M) to block the contribution of the other Na^+ -dependent glutamate/aspartate transporter GLAST, which is also expressed, albeit at low levels, in primary astrocytes (Abrahamsen et al., 2013) (Figure 3a). In both control and *Rest*-KO astrocytes, glutamate uptake was strongly depressed in the presence of choline and almost completely inhibited by TBOA, clearly indicating the major contribution of GLT-1 to the uptake mechanism (Figure 3b). Glutamate uptake was significantly lower in *Rest*-KO astrocytes compared to control cells, consistent with the possibility of an impaired function of Kir4.1 channels. Notably, Ba^{2+} significantly inhibited glutamate

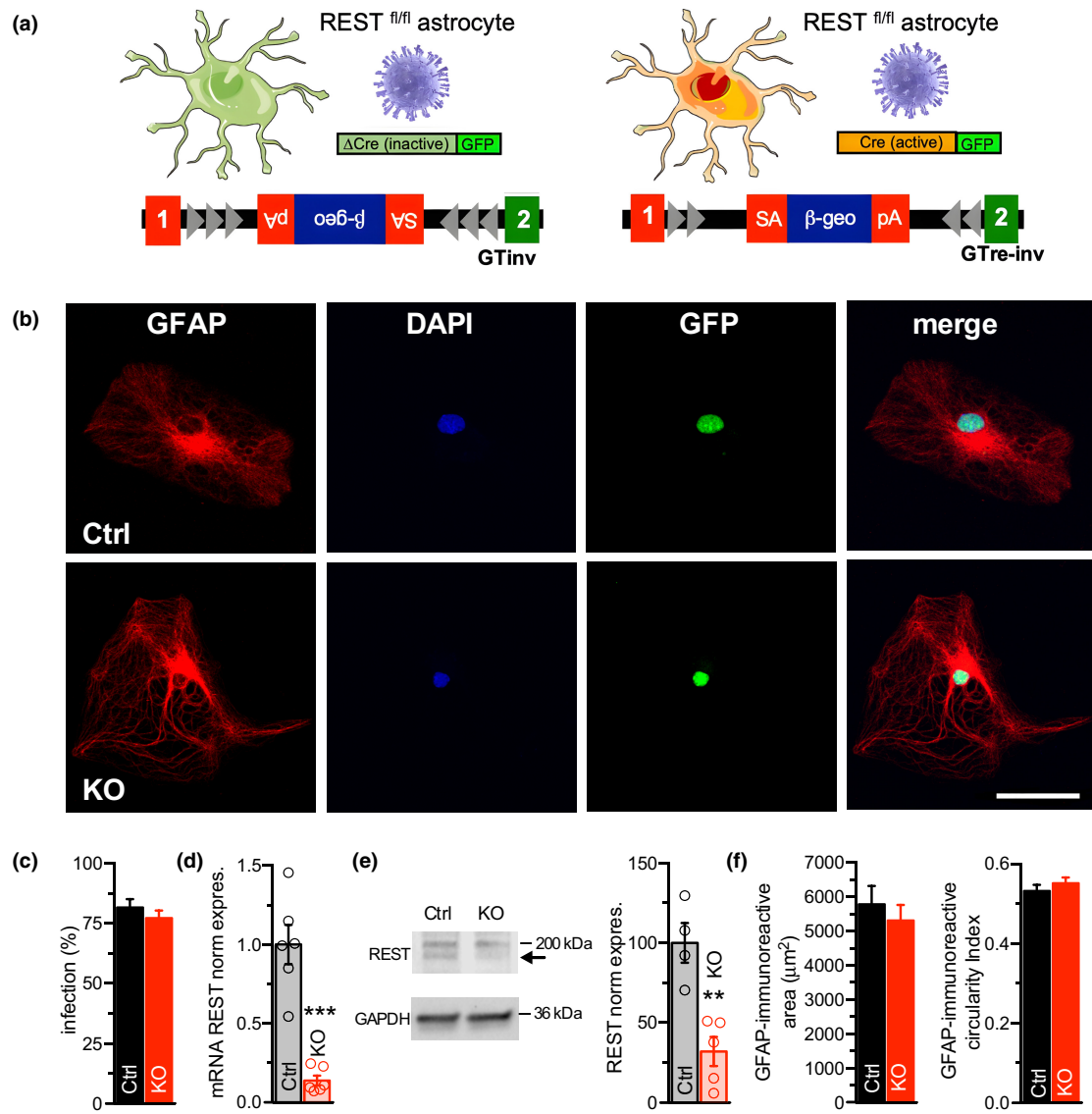


FIGURE 1 *Rest* deletion does not change the morphology of primary astrocytes. (a) *Rest* deletion strategy. Primary astrocytes from $REST^{GTi}$ mice bearing an inverted GT cassette between exons 1 and 2 (GTinv; Nechiporuk et al., 2016) were transduced with lentiviral vectors encoding either active Cre recombinase fused to nuclear GFP (*Rest*-KO astrocytes, right) or a GFP-fused, inactive deletion mutant of Cre recombinase (Δ Cre; control astrocytes, left). (b) Representative images of GFAP immunostaining (red) in primary control and *Rest*-KO astrocytes (25 DIV). DAPI staining was used to label cell nuclei (blue) and nuclear GFP (green) as reporter of infected cells. Merge panels on the right represent the superimposition of all images. Scale bar, 20 μ m. (c) Mean (\pm sem) percentage of astrocytes infected with either Δ Cre (Ctrl) or Cre (KO) encoding lentiviral vectors ($n = 22$ coverslips from 3 independent preparations; Student's *t*-test, $df = 37$, t -value = 0.9276, $p = 0.3596$). The high transduction efficiency (75%–80%) did not differ between the two experimental groups. (d, e) Mean \pm sem *Rest* mRNA (d) and protein (e) levels evaluated in control and *Rest*-KO astrocytes by real-time qPCR ($n = 10$ independent preparations; *** $p < 0.001$, Student's *t*-test, $df = 10$, t -value = 6.738, $p = 0.0001$) and western blotting ($n = 5$ different cultures from three independent preparations; ** $p < 0.01$, Student's *t*-test, $df = 7$, t -value = 4.501, $p = 0.0028$) respectively. The arrow indicates the specific REST band in the representative immunoblot. (f) Morphological analysis of GFAP expression in control and *Rest*-KO astrocytes. The bar graphs represent the mean (\pm sem) GFAP immunoreactive area (left) and circularity index (right) calculated for control ($n = 178$) and *Rest*-KO ($n = 176$) astrocytes from three independent preparations. Left: Student's *t*-test, $df = 352$, t -value = 0.664, $p = 0.5071$; right: Student's *t*-test, $df = 352$, t -value = 0.9229, $p = 0.3567$.

uptake in control astrocytes, but its effect was fully occluded in *Rest*-KO astrocytes (Figure 3b).

To get an independent demonstration of the impaired glutamate uptake by *Rest*-KO astrocytes, we measured glutamate-evoked currents in astrocytes of both phenotypes in the presence of blockers of GLAST (UCPH) and ionotropic glutamate receptors (CNQX and

AP5, 10 and 50 μ M respectively). Glutamate uptake is coupled to a reversible inward Na^+ current evoked in astrocytes clamped at -70 mV and challenged with L- glutamate (1 mM; Bergles & Jahr, 1997). In agreement with the 3H -Glu uptake assay, *Rest*-KO astrocytes exhibited glutamate-evoked, TBOA-sensitive inward currents that were significantly decreased compared to control astrocytes (Figure 3c).

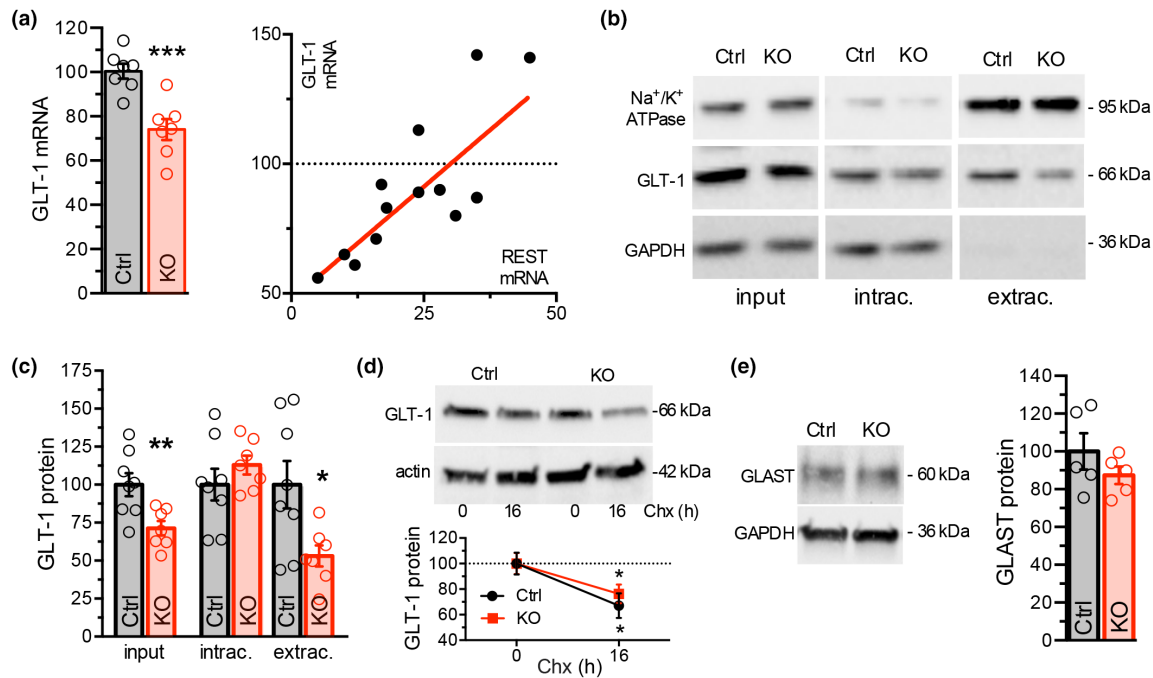


FIGURE 2 The expression of GLT-1, but not of GLAST, is decreased in REST-deleted astrocytes. (a) *Left*: GLT-1 mRNA levels evaluated by real-time qPCR in control and *Rest*-KO astrocytes ($n = 4$ independent preparations) $***p < 0.001$, Student's *t*-test, $df = 12$, t -value = 4.487, $p = 0.0007$. *Right*: Correlation between the extent of *Rest* knockdown obtained in primary astrocytes by changing the multiplicity of infection and the GLT-1 mRNA levels. Pearson's correlation coefficient: 0.76, $p < 0.001$ ($n = 14$ independent preparations). (b) Representative immunoblots of cell surface biotinylation performed in control and *Rest*-KO primary astrocytes cultures. The total expression of GLT-1 protein (input) was analyzed by immunoblotting together with the biotinylated (extracellularly exposed at the cell surface; ext) and non-biotinylated (intracellular; in) GLT-1 fractions. Na^+/K^+ -ATPase and GAPDH were included as markers of plasma membrane and cytosolic fractions, respectively. Input and intracellular fractions represent 5% of the original samples. (c) Quantitative analysis of the biotinylation experiments. The total expression of GLT-1 protein in decreased by REST deletion, consistent with the mRNA changes, and the decrease translates into a net decrease of the membrane targeted fraction. The data were normalized to the mean value of control astrocytes and expressed as means \pm sem ($n = 8$ and 7 for control and *Rest*-KO astrocytes, respectively, from three independent preparations). The percentage of biotinylated protein was 12.7 ± 2.5 for control and 7.6 ± 0.9 for *Rest*-KO cells. Unpaired Student's *t*-test: Input: $**p < 0.01$, $df = 13$, t -value = 3.102, $p = 0.0084$; intrac.: $df = 13$, t -value = 1.025, $p = 0.324$; extrac.: $*p < 0.05$, $df = 13$, t -value = 2.610, $p = 0.0216$. (d) GLT-1 protein turnover in control and *Rest*-KO astrocytes ($n = 4$ independent preparations; Ctrl: $*p < 0.05$, unpaired Student's *t*-test, $df = 19$, t -value = 2.534, $p = 0.0202$; KO: $*p < 0.05$, unpaired Student's *t*-test, $df = 20$, t -value = 2.113, $p = 0.0474$). Astrocytes were harvested before (0 h) and 16 h after treatment with cycloheximide (Chx; 50 $\mu\text{g}/\text{mL}$) and subjected to immunoblotting for GLT-1. *Top*: Representative immunoblots. *Bottom*: Quantitative analysis of GLT-1 turnover. Data were normalized to the mean value of the respective experimental group before Chx treatment (0 h) and expressed as means \pm sem (0 h: $n = 10$ and 13; 16 h: $n = 16$ and 16 different cultures for control and *Rest*-KO astrocytes, respectively, from five independent preparations). $*p < 0.05$ at 16 h, unpaired Student's *t*-test, $df = 20$, t -value = 2.113, $p = 0.0474$. (e) Representative immunoblot (*left*) and quantitative analysis (*right*) of the GLAST protein levels evaluated in control and *Rest*-KO astrocytes by western blotting. Data were normalized to the mean value of control astrocytes and expressed as means \pm sem ($n = 5$ different cultures for both control and *Rest*-KO astrocytes from three independent preparations; unpaired Student's *t*-test, $df = 8$, t -value = 1.206, $p = 0.2623$).

Altogether these data indicate that *Rest*, notwithstanding its main activity of transcriptional repressor, favors the transcription of GLT-1. Moreover, the lack of inhibition of glutamate transport by Ba^{2+} suggests that a potential involvement of Kir4.1 potassium channels can be associated with and contribute to the glutamate uptake phenotype.

3.4 | *Rest* deletion in primary astrocytes down-regulates an inward-rectifier potassium current

To address an involvement of K^+ conductances, we next sought to determine whether the presence of REST influences the passive

membrane properties and whole-cell membrane conductance of primary astrocytes. Macroscopic currents were recorded by the whole-cell patch clamp technique in control and *Rest*-KO cells. Compared to control astrocytes *Rest*-KO cells displayed a significantly more depolarized resting membrane potential (V_{rest}) (Figure 4a). To address the possibility that the more positive V_{rest} could be because of a change in the resting membrane conductance, astrocytes were stimulated with slow voltage ramps. Cells were voltage clamped at the holding potential (V_h) of -70mV , and then hyperpolarized for 200ms at -100mV to reach a steady conductance before applying a slow depolarizing ramp to 80mV (Figure 4b, inset). Compared to *Rest*-KO astrocytes, control cells displayed increasing inward currents at membrane potentials

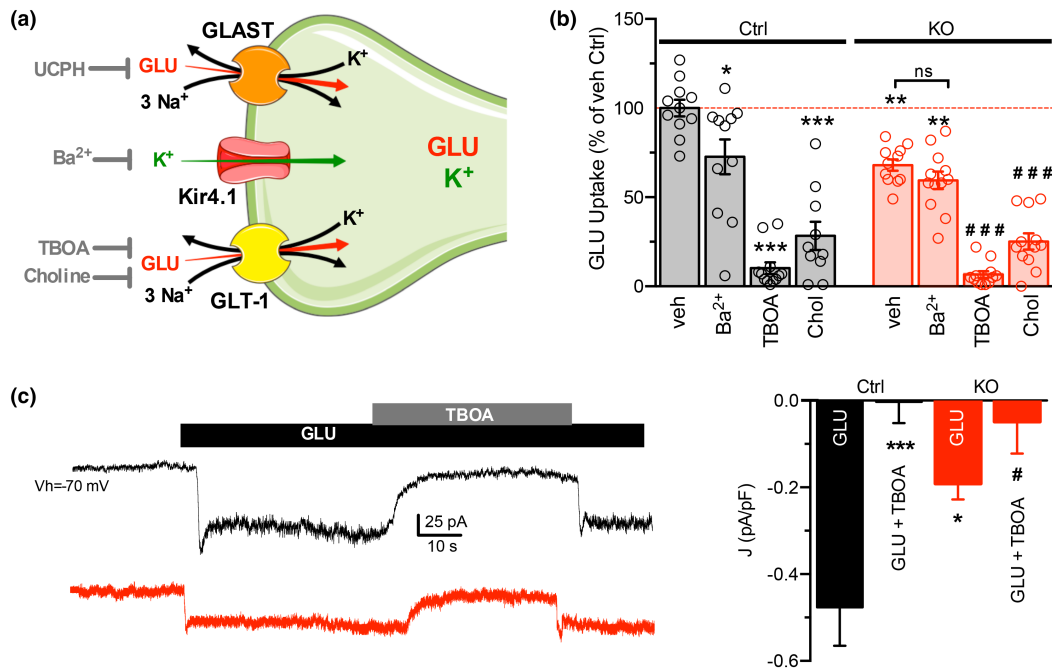


FIGURE 3 Glutamate uptake is impaired in astrocytes deleted for *Rest*. (a) Schematics of the ³H-glutamate uptake experiments. All assays were performed in the presence of UCPH (10 μM) to block GLAST. Treatments to assess specificity of the transport and its dependency on Kir4.1 included the GLT-1 inhibitor TBOA (100 μM) or vehicle (veh) thereof, the Kir4.1 blocker Ba²⁺, and the replacement of extracellular Na⁺ with choline. (b) Quantitative analysis of ³H-glutamate uptake by control (Ctrl) and *Rest*-KO astrocytes (21–24 DIV; 11–12 independent preparations). Data (means ± sem) were normalized to the mean value of control astrocytes. **p* < 0.05, ***p* < 0.01, ****p* < 0.001 versus veh/ Ctrl group; ###*p* < 0.01, ####*p* < 0.001 versus veh/*Rest*-KO group; one-way ANOVA/Bonferroni's tests (*n* = 4 independent preparations; *F*(7, 83) = 38.6; *p*-values: veh Ctrl vs. Ba²⁺ Ctrl: *p* = 0.0195; veh Ctrl vs. TBOA Ctrl: *p* = 0.0001; veh Ctrl vs. Choline Ctrl: *p* = 0.0001; veh Ctrl vs. veh KO: *p* = 0.0025; veh Ctrl vs. Ba²⁺ KO: *p* = 0.0001; veh KO vs. Ba²⁺ KO: *p* = 0.9999; veh KO vs. TBOA KO: *p* = 0.0001; veh KO vs. Choline KO: *p* = 0.0001). (c) *Left*: Representative transport current traces obtained during whole-cell voltage-clamp recordings from control (black) and *Rest*-KO (red) astrocytes clamped at V_h of -70 mV. The L-glutamate (1 mM) evoked inward currents were completely blocked by 100 μM TBOA. *Right*: Analysis of the glutamate transport current density (*J*) recorded in control (Ctrl) and *Rest*-KO astrocytes, with an external solution containing L-Glutamate in the absence or presence of TBOA. ****p* < 0.001, GLU Ctrl versus TBOA GLU Ctrl, Wilcoxon test, *p* = 0.0001; **p* < 0.05, GLU KO vs TBOA KO, Wilcoxon test, *p* = 0.0391; #*p* < 0.05, GLU Ctrl versus GLU KO, Mann-Whitney *U*-test, *p* = 0.0337 (*n* = 18 and 8 for control and *Rest*-KO astrocytes respectively).

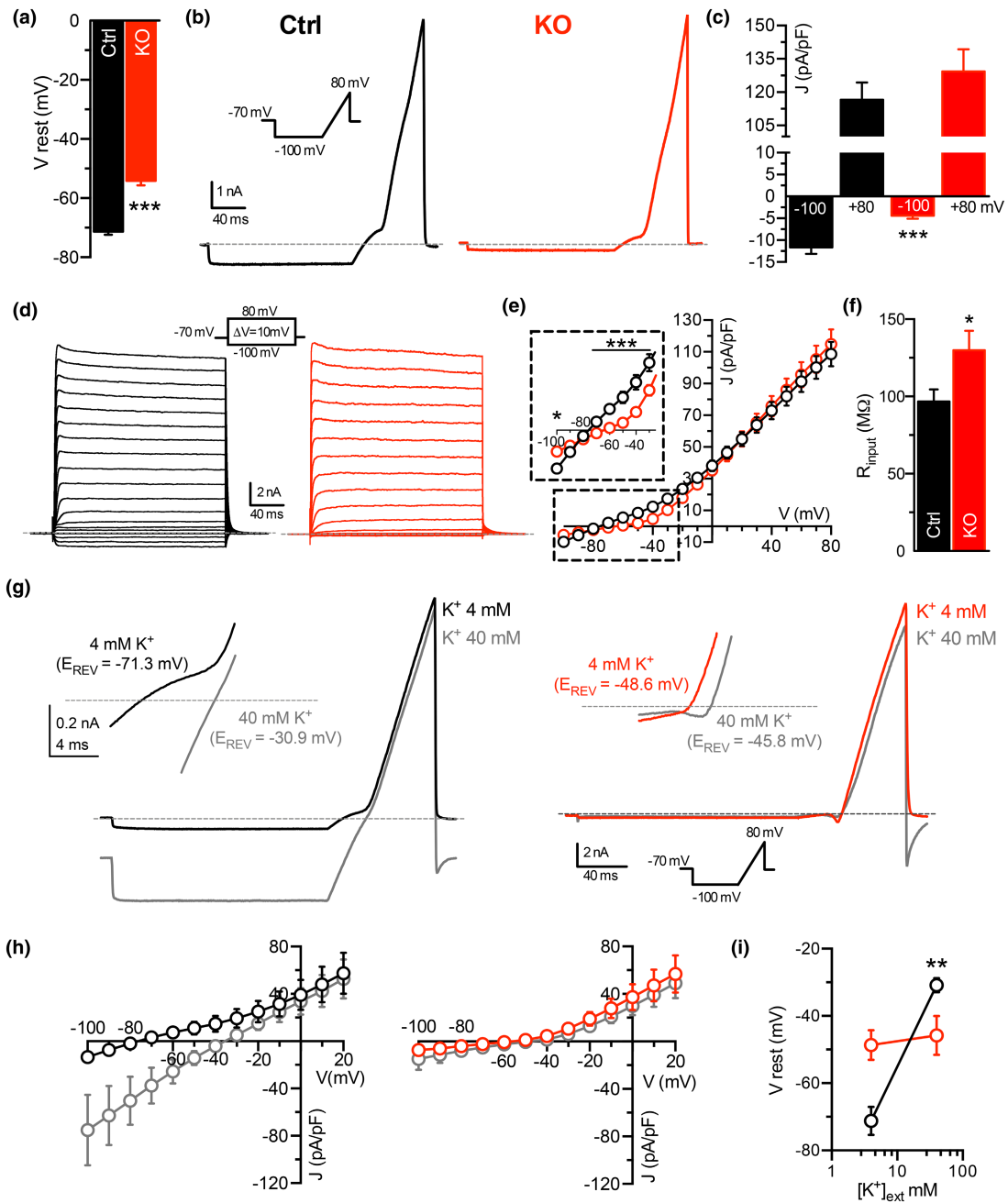
below V_{rest} (Figure 4b). The mean current densities (*J* = pA/pF) at -100 and 80 mV in control and *Rest*-KO astrocytes confirmed that, while the membrane conductance at 80 mV was not significantly different in the presence or absence of REST at -100 mV, it was more than twofold lower in *Rest*-KO astrocytes (Figure 4c).

We next addressed the voltage-dependent kinetics of membrane currents activated under the two conditions. Astrocytes were stimulated with a family of 200-ms voltage steps (with 10-mV increments) from V_h of -70 mV (Figure 4d, inset). Control and *Rest*-KO astrocytes exhibited identical quasi-instantaneous positive currents at potentials above -70 mV. By contrast, sustained non-inactivating negative currents were triggered at potentials below -70 mV only in control astrocytes (Figure 4D,e). The lack of inward current in *Rest*-KO astrocytes was paralleled by an increase in input resistance (R_{input}, Figure 4f). Collectively, these results demonstrate that primary astrocytes in which *Rest* is knocked out exhibit a more depolarized V_{rest} and an increase in R_{input} associated with the absence of inward currents activated at negative membrane potentials. The above results suggest that *Rest* is necessary for the expression of a large resting conductance likely mediated by K⁺ flux that determines the negative V_{rest} in control cells. To corroborate

this view, electrophysiological experiments were carried out under various extracellular K⁺ concentrations (K⁺_{ext}). Elevation of K⁺_{ext} from 4 to 40 mM in control astrocytes evoked a ~40 mV positive shift in the current reversal potential (E_{rev}) but did not affect the E_{rev} of *Rest*-KO cells. Notably, the shift in reversal potential was accompanied by an augment in chord conductance at negative potentials (Figure 4g, left), a result that was virtually absent in *Rest*-KO astrocytes (Figure 4g, right). The current-voltage relationship of currents evoked with the voltage step protocol confirmed these results (Figure 4h). Finally, in control astrocytes, but not in *Rest*-KO cells, V_{rest} was positively shifted by 40 mV (Figure 4i). Collectively, these results indicate that astrocytic *Rest* regulates the functional expression of an inward rectifier K⁺ conductance, which has a relevant role in setting V_{rest}.

3.5 | The Kir4.1 channel mediates the resting potassium conductance functionally regulated by *Rest*

To identify the K⁺ channel subtype functionally regulated by *Rest*, we took advantage of a pharmacological signature that allows to



differentiate the type of resting K^+ current expressed in astrocytes. Indeed, it is well known that astrocytes express inward rectifier (Kir) channel subtype 4.1 both in vivo and in vitro (Benfenati et al., 2006; Hibino et al., 2004, 2010; Li et al., 2001; Olsen et al., 2015; Seifert et al., 2009), but also open rectifier two-pore domains K^+ channels (K_{2p}) (Ryoo & Park, 2016). The most relevant pharmacological feature for distinguishing Kir from K_{2p} conductance is the full blockade of Kir4.1 by low micromolar concentrations of extracellular Ba^{2+} , which does not affect K_{2p} currents (Ferroni et al., 1995; Olsen et al., 2006; Zhou et al., 2009). In control astrocytes, the extracellular administration of Ba^{2+} (200 μ M) resulted in the complete inhibition of the negative ramp currents, while leaving unaltered the positive current evoked at depolarized potentials (Figure 5a, left). By contrast,

in Rest-KO astrocytes, the effect of Ba^{2+} on the ramp current was negligible (Figure 5a, right). These results were corroborated by the quantitative analysis of the Ba^{2+} effect on currents evoked by the voltage-step protocol (Figure 5b,c).

As a further indication that Rest controls the functional expression of Kir4.1, we addressed the effect of interleukin-1 β (IL-1 β), previously showed to inhibit Kir4.1-mediated current in astrocytes (Zuolo et al., 2012). After a preliminary check by RT-PCR that Rest deletion did not affect the expression of the IL-1 β receptor, which is not a Rest target, we incubated astrocytes of either genotype with IL-1 β (10 ng/mL) for 24h. While the kinetics of outward currents were not significantly affected in both genotypes, IL-1 β induced a strong reduction of the inward current only in control astrocytes functionally expressing Kir

FIGURE 4 Rest deletion decreases the astrocyte inward-rectifier K^+ conductance. (a) Rest-deleted astrocytes (KO; $n = 100$ cells) show a more positive resting membrane potential compared to control (Ctrl; $n = 116$ cells) astrocytes. $***p < 0.001$, Mann-Whitney test, $p < 0.0001$. (b) Representative inward/outward rectifying currents recorded in control (black) and Rest-KO (red) astrocytes evoked by a voltage ramp protocol from a V_h of -70 mV (inset). (c) Ramp current densities (J) at -100 and 80 mV show a sustained reduction of inward current in Rest-KO astrocytes ($n = 102$ cells) with respect to control astrocytes ($n = 116$ cells). 80 mV: Ctrl versus KO, Mann-Whitney U-test, $p = 0.6709$; $***p < 0.001$, -100 mV: Ctrl versus KO, Mann-Whitney test, $p = 0.0001$. (d) Representative family of voltage- and time-dependent membrane currents evoked by voltage steps (inset). Non-inactivating inward currents were recorded only in control astrocytes. (e) J/V relationship of the evoked currents for control and Rest-KO astrocytes shows the same level of outward current in both genotypes and a marked reduction of the inward component in Rest-KO astrocytes (inset). $*p < 0.05$, -100 mV: Ctrl vs KO, Mann-Whitney's U-test, $p = 0.0152$; $***p < 0.001$, from -70 to -35 mV, Mann-Whitney's U-test, $p = 0.0001$. (f) The input resistance, calculated for both genotypes, shows an increase in Rest-KO astrocytes ($n = 91$ cells) with respect to control astrocytes ($n = 100$ cells). $*p < 0.05$, Mann-Whitney test, $p = 0.0249$. All data are expressed as means \pm sem. (g) Representative current traces of control (Ctrl; black) and Rest-KO (red) astrocytes evoked in 4 and 40 mM extracellular K^+ ($[K^+]_{ext}$; gray) by replacing the ion with equimolar concentrations of Na^+ . The increase in $[K^+]_{ext}$ positively shifts the reversal potential (E_{rev}) of the current in control, but not in Rest-KO, astrocytes. The shift in E_{rev} to more positive potentials is accompanied by a reduction of its rectifying profile, which indicates the activation of an inward-rectifier K^+ channel that approximates the behavior predicted by the constant field theory for simple K^+ electrodiffusion. (h) J/V plot of steady-state currents evoked in 4 and 40 mM of $[K^+]_{ext}$ with a voltage step protocol in control (black) and Rest-KO (red) astrocytes. The E_{rev} shifts and the reduction of the rectifying profile induced by high $[K^+]_{ext}$ (gray), clearly visible in control astrocytes, are virtually absent in Rest-KO astrocytes. (i) Shifts in V_{rest} in control ($n = 9$ cells) and Rest-KO ($n = 9$ cells) astrocytes by rising $[K^+]_{ext}$ from 4 to 40 mM. $**p < 0.01$, K^+ 4 mM Ctrl vs K^+ 40 mM Ctrl, Wilcoxon's matched pairs signed rank test, $p = 0.0039$; K^+ 4 mM KO vs K^+ 40 mM KO, Wilcoxon's matched pairs signed rank test, $p = 0.5469$. All data are expressed as means \pm sem.

current (Figure 5d,e), a result which was reflected by V_{rest} decrease in this astrocyte population (Figure 5f). Similar findings were obtained by the analysis of the current density evoked by the voltage step protocol that clearly showed a full occlusion of the effects of IL-1 β in Rest-KO astrocytes (Figure 5g). Altogether, these results strongly suggest that in primary astrocytes the presence of Rest is necessary for the functional expression of Kir4.1-mediated resting K^+ conductance.

3.6 | Rest deletion decreases membrane targeting, but not total expression levels, of Kir4.1 channels

To dissect the molecular basis of the biophysical and pharmacological results, we analyzed the expression levels of Kir4.1 mRNA and protein in both control and Rest-KO astrocytes by RT-PCR and western blotting. In contrast with the functional defect in Kir4.1 currents observed in Rest-KO astrocytes, the total mRNA and protein levels of Kir4.1 were not affected by Rest deletion (Figure 6a), consistent with the fact that *Kcnj10* is not a direct REST target gene. Thus, we considered the possibility that the intracellular trafficking of the channel and/or its subcellular compartmentalization could be indirectly affected by Rest deletion.

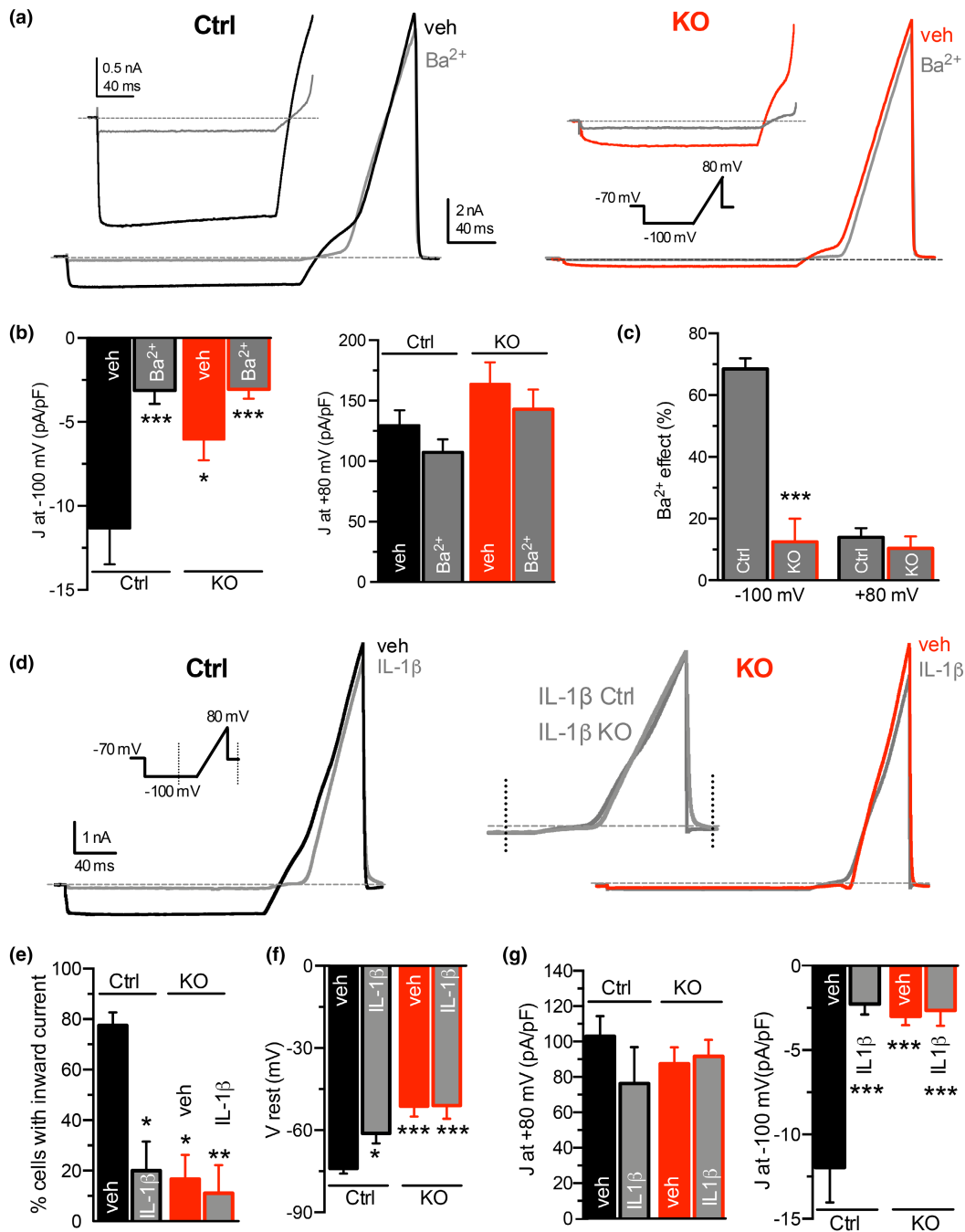
To this aim, we run surface biotinylation experiments to quantify, by streptavidin affinity pull-down, the ratio between the functional channels exposed at the plasma membrane surface and those retained intracellularly (Figure 6b). Interestingly, the surface expression of Kir4.1 on the plasma membrane was significantly decreased, while the intracellular pool of the channel was correspondingly increased (Figure 6c).

This finding is consistent with the biophysical and pharmacological results described above and indicates that the impaired glutamate uptake of Rest-KO astrocytes is linked to the observed downregulation of Kir4.1 channels, confirming the important

contribution of Kir4.1 activity to the Na^+ -dependent glutamate uptake (Shimamoto et al., 1998). Since GLT-1 and Kir4.1 are known to form supramolecular complexes in discrete spots on astrocyte processes (Higashi et al., 2001; Murphy-Royal et al., 2015; Schreiner et al., 2014), the fall in membrane GLT-1 can be potentially responsible for the impaired targeting or decreased permanence of Kir4.1 channels at the plasma membrane observed in Rest-KO astrocytes.

3.7 | Neurons co-cultured with Rest-KO astrocytes display an altered firing phenotype

We next sought to determine whether the described changes in the expression of relevant astrocyte homeostatic proteins in Rest-KO astrocytes could affect the neuronal function in terms of single-cell excitability. To this end, wild-type hippocampal neurons were co-cultured with control or Rest-KO astrocytes for 14 days before performing patch-clamp measurements of intrinsic excitability in visually identified excitatory pyramidal neurons (Figure 7a; Watt et al., 2000; Prestigio et al., 2019). Neurons co-cultured with either control or Rest-KO astrocytes showed no alteration in V_{rest} and input resistance (Figure 7b,c). Moreover, they responded to the injection of depolarizing current-steps (1-s duration of 10 pA increasing amplitude) by firing evoked action potentials (APs) with no overt differences in the minimum current necessary to evoke the first AP (rheobase; Figure 7d,e). However, the analysis of the instantaneous firing frequency revealed that Rest deletion in astrocytes strongly increased the high-frequency firing activity evoked by intense depolarizing currents in wild-type co-cultured neurons, as compared to neuronal cocultures with control astrocytes (Ctrl-N; Figure 7f). This increased hyperactivity of wild-type neurons cultured with Rest-KO astrocytes was confirmed by the significantly higher number of APs



evoked by injection of 1 s-step of 300 pA of depolarizing current with respect to neurons co-cultured with control astrocytes (Figure 7g).

Finally, the analysis of the waveform of the first AP evoked by minimal current injection showed that neurons co-cultured with astrocytes of both genotypes exhibited the similar amplitude, maximal rising slope and threshold of activation. However, wild-type neurons co-cultured with Rest-KO astrocytes experienced a decreased amplitude of after-hyperpolarization, a phase that strictly depends on the extracellular K^+ concentration (Figure 7h,i). Collectively, these results suggest that the impaired function of Kir4.1 channels in Rest-KO astrocytes impacts on the K^+ buffering activity, increasing the excitability of co-cultured neurons in periods of intense electrical activity.

3.8 | Neurons co-cultured with Rest-KO astrocytes display strengthened excitatory synaptic transmission

Since we have shown that Rest deletion in astrocytes impairs GLT-1 expression and functionality, we tested the hypothesis that a decreased glutamate clearance in the synaptic environment by perisynaptic astrocytes could affect excitatory synaptic strength. To this end, we studied the miniature excitatory postsynaptic currents (mEPSCs) in wild-type neurons co-cultured with control or Rest-KO astrocytes (Figure 8a). While the mEPSC amplitude reflects the quantal size of neurotransmitter (neurotransmitter content of single synaptic vesicles and postsynaptic receptor sensitivity), the mEPSC frequency depends on the

FIGURE 5 The inward-rectifier K^+ current down-regulated by *Rest* deletion is mediated by Kir4.1 channels. (a) Representative ramp current traces elicited in control (Ctrl; black) and *Rest*-KO (red) astrocytes before and after acute treatment with extracellular solution containing Ba^{2+} ($200\mu M$; gray). A higher magnification of currents at negative potentials is shown (*inset*). (b) Current density (J) recorded at -100 (left) and 80 (right) mV in both genotypes in the absence or presence of Ba^{2+} as in A. (c) The net percent effect of Ba^{2+} at -100 and 80 mV shows the selective full blockade of inward current in control astrocytes and the full occlusion of the effect by *Rest* deletion in *Rest*-KO astrocytes. All data are expressed as means \pm sem ($n = 51$ and 45 cells for control and *Rest*-KO astrocytes respectively). $*p < 0.05$, $***p < 0.001$, two-way ANOVA/Bonferroni's tests, treatment \times genotype $F(1, 94) = 29.49$, Ctrl veh versus KO veh: $p = 0.041$; Ctrl veh versus Ctrl Ba^{2+} , $p = 0.0001$; KO veh versus KO Ba^{2+} , $p = 0.051$. (b, left panel), $***p < 0.001$, -100 mV: Ctrl versus KO, Mann-Whitney's U -test, $p = 0.0001$; 80 mV: Ctrl versus KO, Mann-Whitney's U -test, $p = 0.6332$ (c). (d) Representative ramp current recordings in control (Ctrl; black) and *Rest*-KO (red) astrocytes treated for 24 h with either vehicle (veh) or IL1 β (10 ng/mL; gray). (e) Percentage of control and *Rest*-KO astrocytes exhibiting inward current before and after treatment with IL1 β (current threshold: -500 pA; $n = 3$ independent experiments). $*p < 0.05$; $**p < 0.01$, one-way ANOVA/Bonferroni's tests, $F(3, 8) = 10.21$, Ctrl veh versus Ctrl IL1 β , $p = 0.0121$; Ctrl veh versus KO veh, $p = 0.0109$; Ctrl veh versus KO IL1 β , $p = 0.0077$. (f) Membrane potential in control and *Rest*-KO astrocytes before and after treatment with IL1 β . IL1 β depolarizes the membrane potential of control astrocytes, while its effect is completely occluded in the already depolarized *Rest*-KO astrocytes. $*p < 0.05$; $***p < 0.001$, one-way ANOVA/Bonferroni's tests, $F(3, 64) = 10.19$, Ctrl veh versus Ctrl IL1 β , $p = 0.0448$; Ctrl veh versus KO veh, $p = 0.0001$; Ctrl veh versus KO IL1 β , $p = 0.0001$. (g) Current density (J) recorded at -100 (left) and 80 (right) mV for both genotypes in the absence (veh) or presence of IL1 β . $***p < 0.001$, one-way ANOVA/Bonferroni's tests, $F(3, 59) = 11.68$, Ctrl veh versus Ctrl IL1 β , $p = 0.0001$; Ctrl veh versus KO veh, $p = 0.0002$; Ctrl veh versus KO IL1 β , $p = 0.0001$ ($n = 22$ and $n = 16$ for vehicle and IL1 β in control astrocytes, respectively; $n = 15$ for both vehicle and IL1 β in *Rest*-KO astrocytes). All data are expressed as means \pm sem.

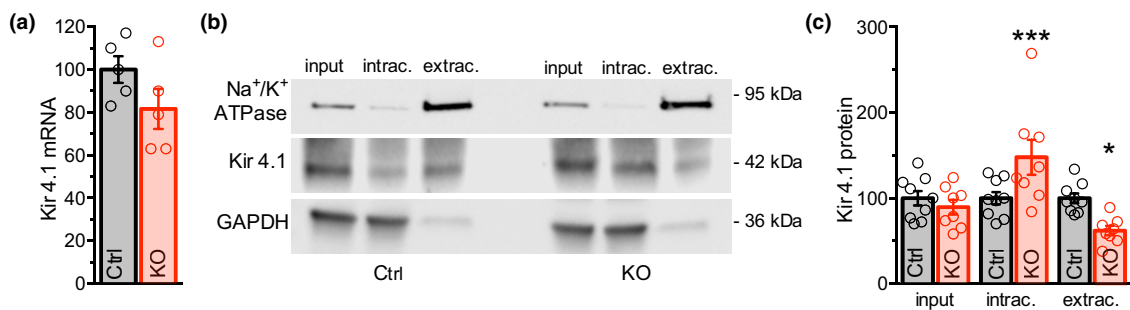


FIGURE 6 *Rest* deletion is associated with an impaired targeting of Kir4.1 channels to the plasma membrane. (a) Kir4.1 mRNA levels evaluated by real-time qPCR in control (Ctrl) and *Rest*-KO astrocytes. No significant changes in the total Kir4.1 transcript levels were detected. Student's t -test, $df = 8$, t -value = 1.635 , $p = 0.1407$. (b) Representative immunoblots of cell surface biotinylation performed in control and *Rest*-KO primary astrocytes cultures. The total expression of Kir4.1 protein (input) was analyzed by immunoblotting together with the biotinylated (extracellularly exposed at the cell surface; ext) and non-biotinylated (intracellular; in) fractions of Kir4.1. Na^+/K^+ -ATPase and GAPDH were included as markers of plasma membrane and cytosolic fractions respectively. Input and intracellular fractions represent 5% of the original samples. (c) Quantitative analysis of the biotinylation experiments. Data were normalized to the mean value of control astrocytes and expressed as means \pm sem ($n = 5$ and 6 different cultures for control and *Rest*-KO astrocytes, respectively, from three independent preparations). The percentage of biotinylated protein was 17.2 ± 3.3 for control and 9.3 ± 1.8 for *Rest*-KO cells. $*p < 0.05$, $***p < 0.001$, unpaired Student's t -test: Input: $df = 9$, t -value = 1.329 , $p = 0.2167$; intrac.: $df = 15$, t -value = 2.299 , $p = 0.0363$; extrac.: $df = 15$, t -value = 4.711 , $p = 0.0003$.

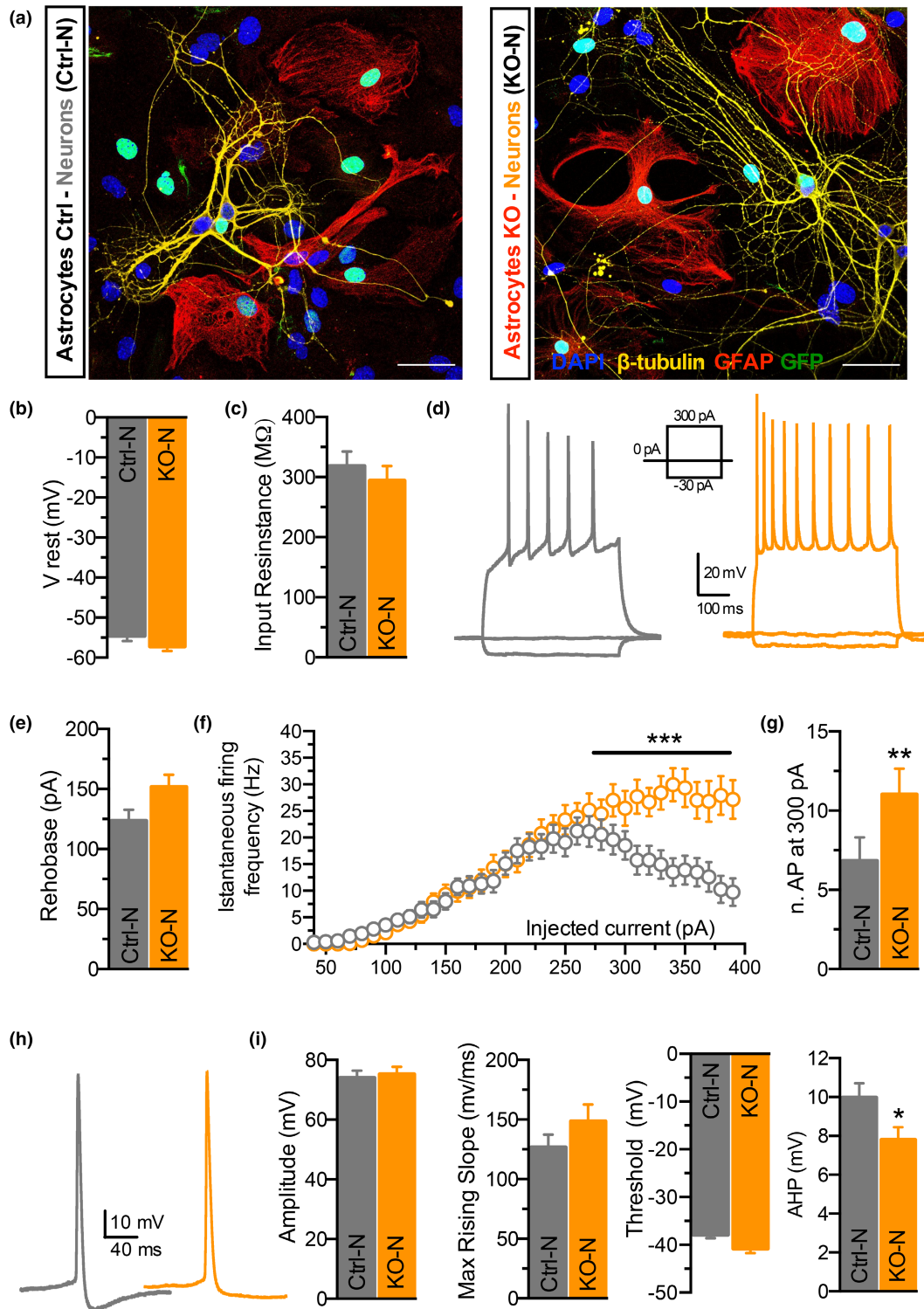
number of active synapses and the probability of spontaneous release of single synaptic vesicles (Stevens, 1993). While mEPSC frequency, charge, decay, and rise times were not significantly altered in neurons co-cultured on astrocytes of either genotype, a significant increase in the mEPSC amplitude was observed when neurons were co-cultured with *Rest*-KO astrocytes (Figure 8b,c). The observed increase in amplitude may reflect a more intense postsynaptic effect of single glutamate quanta that, in the absence of changes in neuronal properties, can be attributed to a lower clearance of the released glutamate by perisynaptic *Rest*-KO astrocytes.

All the above results suggest that the *Rest* deletion, which leads to impaired astrocytic ability to buffer K^+ and glutamate via Kir4.1 and GLT-1, causes an increased intrinsic excitability that emerges under conditions of intense electrical activity, and at the same time,

potentiates the effect of the released glutamate by increasing the excitatory synaptic strength.

4 | DISCUSSION

Rest was initially known for its ability to repress the expression of neuronal genes in non-neuronal cells (Chong et al., 1995; Schoenherr et al., 1996), such as astrocytes, where it orchestrates the lineage and maintains the astrocytic phenotype by repressing the expression of neuron-specific genes containing the RE-1 binding site (Abrajano et al., 2009a, 2009b; Ballas et al., 2005; Kohyama et al., 2010). Here, we have studied if *Rest* deletion affects the physiology of astrocytes and how this deletion impacts on neuronal network homeostasis.



While conventional brain-specific *Rest* KO lines (Gao et al., 2011) targeting *Rest* exon 2 still express a C-terminal REST peptide, we used in this study the *Rest*-KO mouse containing a conditional gene trap cassette in an intron of the endogenous *Rest* gene that terminates transcription upstream from the initiator codon (Nechiporuk et al., 2016). Moreover, to avoid the compensatory effects elicited by chronic gene deletion, we switched off the *Rest* gene in primary astrocytes using lentiviruses expressing Cre recombinase.

Astrocytes contribute to maintaining neuronal homeostasis by buffering ions/molecules that are released during normal and sustained firing activity and synaptic transmission (Haydon, 2001; Theodosis et al., 2008). Astrocytes control the $[K^+]_{ext}$ homeostasis by Kir channels, avoiding the hyperexcitation of the neuronal network associated with increased extracellular K^+_{ext} (Kofuji & Newman, 2004) and the levels of extracellular glutamate at synaptic sites by expressing glutamate transporters that prevent

FIGURE 7 Primary neurons co-cultured with *Rest*-KO astrocytes display an enhanced intrinsic excitability. (a) Representative merged images of hippocampal neurons (14 DIV) co-cultured with control (Ctrl-N) and *Rest*-KO astrocytes (KO-N). Cells were immunostained with DAPI (blue, nuclei), β -tubulin (yellow, neurons), GFAP (red, astrocytes), and GFP (green, transduced astrocytes). Scale bar, 45 μ m. (b, c) The neuronal resting membrane potential (b) and the input resistance (c) were not significantly different between the two experimental groups. Mann-Whitney *U*-test, $p = 0.1644$ (b); $p = 0.4217$ (c). (d) Representative current-clamp recordings of neuronal action potentials (APs) induced by the injection of -30, 0 and +300 pA steps for 1 s in Ctrl-N (gray) and KO-N (orange). (e) The rheobase (current to reach the threshold voltage for the first AP) is not significantly different between neurons co-cultured with either control or *Rest*-KO astrocytes. Mann-Whitney *U*-test, $p = 0.0516$. (f) Instantaneous firing frequency as a function of injected current for Ctrl-N and KO-N phenotypes. Neurons co-cultured with *Rest*-KO astrocytes displayed a significantly higher evoked instantaneous firing frequency at the largest current injections (>300 pA). *** $p < 0.001$, Mann-Whitney *U*-test, Ctrl-N vs KO-N, 290 pA: $p = 0.0010$; 300 pA: $p = 0.0008$; 310 pA: $p = 0.0006$; 320 pA: $p = 0.0005$; 330 pA: $p = 0.0003$; 340 pA: $p = 0.0001$; 350 pA: $p = 0.0004$; 360 pA: $p = 0.0010$; 370 pA: $p = 0.0009$; 380 pA: $p = 0.0001$; 390 pA: $p = 0.0001$. (g) Number of APs evoked at 300 pA of current injected for both experimental conditions. ** $p < 0.01$, Mann-Whitney *U*-test, $p = 0.0011$. (h) Representative traces of the shape of the first AP evoked by minimal current injection recorded in Ctrl-N (gray) and KO-N (orange) co-cultured neurons. (i) AP Amplitude, max rising slope, threshold, and after-hyperpolarization (AHP) potentials estimated in neurons co-cultured with either control or *Rest*-KO astrocytes. All data are expressed as means \pm sem with $n = 38$ and 41 neurons co-cultured with control and *Rest*-KO astrocytes respectively. * $p < 0.05$, Mann-Whitney *U*-test, Amplitude: $p = 0.6332$; Max rising slope: $p = 0.3996$; Threshold: $p = 0.0929$; AHP: $p = 0.0326$.

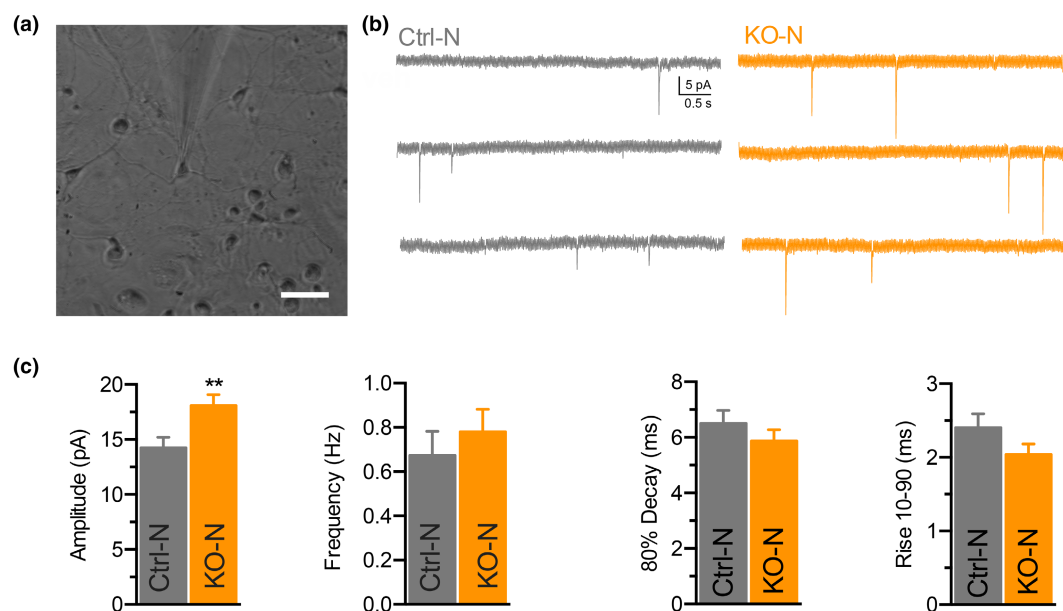


FIGURE 8 Miniature excitatory postsynaptic currents of neurons co-cultured with *Rest*-KO astrocytes reveal a postsynaptic effect of released glutamate. (a) Phase-contrast image of co-cultures of wild-type primary hippocampal neurons with astrocytes. Scale bar, 40 μ m. (b) Representative traces of mEPSCs from neurons co-cultured with either control (Ctrl-N, gray) or *Rest*-KO (KO-N, orange) astrocytes. (c) Analysis of mEPSCs. From *left to right*, mEPSC amplitude, frequency, 80% decay time, and 10%-90% rise time are shown. Data are expressed as means \pm sem with $n = 43$ and 50 for Ctrl-N and KO-N, respectively, from five independent cultures. ** $p < 0.001$, Mann-Whitney *U*-test, Amplitude: $p = 0.0063$; Frequency: $p = 0.4951$; 80% decay time: $p = 0.3380$; 10%-90% rise: $p = 0.1390$.

excessive stimulation of glutamate receptors and glutamate spillover (Sulkowski et al., 2014).

4.1 | REST deletion in astrocytes decreases the expression of glutamate transporter GLT-1

Astrocytes express high levels of two EAATs that localize in the proximity of glutamatergic synapses and perform properly at membrane potentials near the K^+ reversal potential, GLAST and GLT-1, the latter of which is responsible for the 90% of the clearance of glutamate released into the synaptic cleft (Danbolt, 2001). While

Rest deletion did not affect astrocyte development or morphology, it induced a dramatic reduction of the mRNA and protein levels of GLT-1, but not of GLAST. The diminished expression of GLT-1 mRNA and protein that we found in our model is in full agreement with a recent report showing a positive transcriptional effect of *Rest* on the GLT-1 gene through binding the two RE-1 sites present in the GLT-1 promoter (Pajarillo et al., 2021, 2022). Indeed, although the main action of *Rest* is to repress a variety of target genes, the occupancy of promoter RE-1 sites can occasionally induce transcriptional activation (Bersten et al., 2014; Kallunki et al., 1998; Perera et al., 2015).

The down-regulation of the total and membrane expression of GLT-1 in *Rest*-KO astrocytes markedly impaired in glutamate uptake

that was insensitive to Ba^{2+} inhibition through blockade of Kir4.1 channels that, in control astrocytes, decreases the electrochemical gradient driving glutamate uptake. We also found that the impaired glutamate uptake is not exclusively caused by the impairment of Kir4.1 channels, but it is directly attributable to decreased transcription and membrane targeting of GLT-1 in *Rest*-KO astrocytes. The results indicate that the impaired glutamate uptake of *Rest*-KO astrocytes is linked to the observed down-regulation of Kir4.1 channels. Our data confirm the important contribution of Kir4.1 activity to the Na^+ -dependent glutamate uptake (Shimamoto et al., 1998); however, they do not allow to discern which of the two phenomena (decreased targeting of Kir4.1 channels to the membrane and impaired glutamate uptake) is the primary consequence of *Rest* deletion. Since GLT-1 and Kir4.1 that form supramolecular complexes in discrete spots on astrocyte processes (Higashi et al., 2001; Murphy-Royal et al., 2015; Schreiner et al., 2014), the fall in membrane GLT-1 can be responsible for the impaired targeting or decreased permanence of Kir4.1 channels at the plasma membrane observed in *Rest*-KO astrocytes.

4.2 | Kir4.1 is affected by *Rest* deletion without being a canonical *Rest* target gene

Although astrocytes express several Kir channel subtypes, Kir 4.1 is the major pore-forming subunit directly linked to this function, as shown by several data obtained in spinal and cortical astrocytes (Djukic et al., 2007; Neusch et al., 2001; Olsen et al., 2006, 2007). It is also known that Kir4.1 conductance affects the strength of electrogenic glutamate uptake in a dual manner: (i) it sets the level of astrocyte membrane potential, thus providing the driving force for transport; and (ii) it limits the spread of transport-associated electrical signals by providing a large shunt conductance (Djukic et al., 2007; Dvorzhak et al., 2016; Olsen & Sontheimer, 2008; Seifert et al., 2009; Tzingounis & Wadiche, 2007). Accordingly, alterations of ion gradients and membrane depolarization resulting from Kir4.1 dysfunction contribute to the reduced activity of other ion gradient- and voltage-dependent transporters and can occasionally cause transporter reversion with release of glutamate (Bordey & Sontheimer, 1997; D'Ambrosio, 2004). In this respect, it has been shown that knockout or Ba^{2+} -mediated inhibition of Kir4.1 are associated with significant reductions in glutamate transport by GLT-1, providing evidence for the tight coupling of the two transporters (Hibino et al., 2010).

Unlike GLT-1, no canonical RE1 elements are present in the regulatory regions of the *Kcnj10* gene and, accordingly, the expression levels of Kir4.1 were not altered by *REST* deletion. However, the insensitivity to Ba^{2+} inhibition of glutamate uptake brought us to consider that a decrease in GLT-1 resulting from *REST* deletion may affect Kir4.1 targeting to the membrane and function. Indeed, we found that *Rest* deletion is associated with a dramatic reduction of inward current accompanied by a marked depolarization of the membrane potential because of an impairment of a K^+

conductance. As astrocytes are characterized by a highly selective membrane permeability to K^+ and a negative resting potential (Ransom & Goldring, 1973), the positive shifted in V_{rest} , associated with R_{in} increase and reduction of inward current, was interpreted as a specific loss of a Kir4.1-mediated current. In astrocytes, the probability of Kir4.1 opening at V_{rest} is high. This contributes to their negative resting membrane potential near the reversal K^+ potential (Verkhratsky & Steinhäuser, 2000) and to a large portion of K^+ permeability, which, in turn, is required for extracellular K^+ clearance. These findings are reminiscent of previous reports in retinal Muller cells, spinal oligodendrocytes, and complex glia in CA1 *stratum radiatum*, in which a lack of Kir4.1 caused full loss of inward currents and depolarization of the V_{rest} (Djukic et al., 2007; Kofuji et al., 2000; Neusch et al., 2001). The specific impairment of Kir4.1 function was challenged by the specific blocker Ba^{2+} , whose effect was virtually occluded in *Rest*-KO astrocytes. In addition, Kir4.1 activity was impaired in neuroinflammation associated with seizure generation in epilepsies of various etiologies (Aronica et al., 2012; Vezzani et al., 2011; Zurolo et al., 2012). It has been observed that, after *status epilepticus*, a peak in expression of IL1 β in the temporal cortex occurs in concomitance with a strong reduction in Kir4.1 activity, suggesting that IL1 β regulates Kir4.1. Interestingly, *Rest*-KO astrocytes were also insensitive to prolonged treatment with IL1 β , which instead depressed Kir4.1-mediated inward currents in control astrocytes.

The impaired opening probability of Kir4.1 in *Rest*-KO astrocytes suggests that *Rest* indirectly regulates the intracellular trafficking and functional membrane targeting of Kir4.1 at the post-transcriptional level. This result opens the possibility that the primary decrease in the expression of the RE1-containing GLT-1 gene secondarily impairs the membrane targeting and/or the lifetime on the membrane of Kir4.1. This possibility is supported by previous data (Higashi et al., 2001; Murphy-Royal et al., 2015; Schreiner et al., 2014) showing that both Kir4.1 channels and GLT-1 co-distribute in spots on astrocyte processes wrapping glutamatergic synapses by forming supramolecular complexes. To corroborate the view on the close functional dynamics of the two proteins, it was previously shown that Kir4.1 and GLT-1 are both down-regulated in astrocytes subjected to traumatic brain injuries in vivo (Gupta & Prasad, 2013; Olsen et al., 2010).

4.3 | Kir4.1 and glutamate clearance impairment in *Rest*-KO astrocytes increase the excitability of co-cultured neurons

Extracellular K^+ and glutamate clearance are among the fundamental functions of astrocytes, as they prevent hyperexcitability in the neuronal network (Chamberlin et al., 1990; Tureček & Trussell, 2000). An impairment of the Kir4.1 subtype leads to hyperexcitability of the perisynaptic environment and results in seizure susceptibility in both mice and humans, contributing to the pathogenesis of a variety of neurological diseases (Bordey & Sontheimer, 1997;

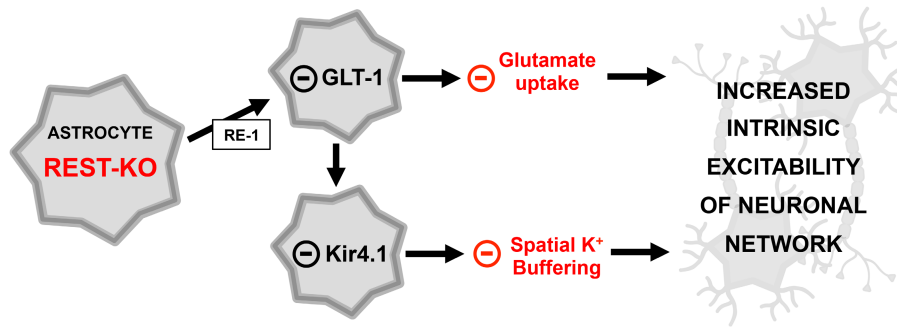


FIGURE 9 Working hypothesis of the indirect effect of REST on spatial K⁺ buffering in astrocytes. Under physiological conditions REST binds to the RE-1 motifs of the *Slc1A2* promoter and stimulates its transcription. GLT-1 is targeted to the astrocyte membrane where it forms a supramolecular complex with Kir4.1. In the absence of REST, the expression of GLT-1 in the cell and on the membrane is decreased with a negative effect on the exposure of Kir4.1 on the membrane. Thus, REST plays a homeostatic role in astrocyte/neuronal networks by directly enhancing extracellular glutamate uptake and indirectly potentiating spatial K⁺ buffering.

Buono et al., 2004; D'Ambrosio et al., 1999; Ferraro et al., 2004; Leis et al., 2005; Nwaobi et al., 2016). Also, a decrease in the expression and/or function of glial glutamate transporters is associated with the epilepsy in humans and GLT-1 deletion in mice leads to seizures and death (Kong et al., 2012; Pajarillo et al., 2019; Petr et al., 2015).

Based on the experimental evidence described above, the dual Kir4.1 and GLT-1 down-regulation in *Rest*-KO astrocytes changes could affect intrinsic excitability and excitatory neurotransmission. Indeed, wild-type neurons co-cultured with *Rest*-deleted astrocytes exhibited impaired after-hyperpolarization potentials following APs and a dramatically increased high-frequency firing activity upon intense depolarization. These results are highly suggestive of an impaired extracellular K⁺ buffering by *Rest*-KO astrocytes that, upon intense and sustained firing activity may induce both intrinsic and network hyperexcitability. The concomitantly impaired glutamate clearance may also alter neuronal network activity by hyperactivating postsynaptic AMPA receptors. Indeed, neurons co-cultured with *Rest*-KO astrocytes display increased mEPSC amplitude, indicative of an increased quantal size of released glutamate because of decreased glutamate clearance by astrocyte perisynaptic endfeet. The impact of this result is noteworthy, since the deficit in GLT-1 can be partially compensated by other glutamate transporters expressed by astrocytes, such as GLAST. However, the latter transporter that normally contributes to a small fraction of glutamate uptake was recently shown not to be affected by *Rest* (Pajarillo et al., 2021).

5 | CONCLUSIONS

Our results demonstrate that *Rest* positively modulates inward K⁺ currents mediated by Kir4.1, notwithstanding the absence of RE-1 binding sites in the Kir4.1 gene promoter. The associated impairment in the expression and function of GLT-1 after REST deletion confirms the positive transcriptional effect of *Rest* on the GLT-1 promoter. Moreover, it offers a molecular explanation for the observed impairment in Kir4.1 function, given that these two membrane actuators work in concert on the astrocyte membrane. This

study adds new insights into the role of Kir4.1 and GLT-1 in astroglial physiopathology. The effects of *Rest* in astrocytes, uncovered by its full deletion, are coherent with an overall homeostatic function in the nervous systems under physiological conditions, in concert with the homeostatic action of neuronal *Rest* (Pozzi et al., 2013; see Baldelli & Meldolesi, 2015). It has been shown that the low levels of *Rest* expression in neurons can be increased by hyperactivity, resulting in a downscaling of intrinsic excitability and excitatory synapses and a concomitant upscaling of inhibitory synapses onto excitatory neurons (Pecoraro Bisogni et al., 2018; Pozzi et al., 2013; Prestigio et al., 2021). Here, we show that the high constitutive levels of *Rest* in astrocytes tonically support GLT-1 expression and Kir4.1 channel exposure on the plasma membrane, in a GLT-1/Kir4.1 supramolecular complex (Figure 9). This reveals a previously unknown role of astrocyte *Rest* in homeostatic plasticity by boosting K⁺ buffering and glutamate clearance, which are the paramount "housekeeping" functions of astrocytes in the brain environment. Such multifaceted homeostatic mechanisms could be exploited as a target for therapies for paroxysmal neurological diseases caused by network hyperexcitability.

AUTHOR CONTRIBUTIONS

EC carried out the electrophysiological experiments in primary astrocytic cultures; MA and AM planned and run the molecular biology and biochemical experiments and analyzed the data under the supervision of AR and FC; TF generated the REST^{G^{Ti}} mouse; PB, SF, PV, and FB conceived the study, analyzed the experimental data, and wrote the manuscript; all authors discussed the experimental results and revised the manuscript.

ACKNOWLEDGMENTS

We are grateful to Gail Mandel (Vollum Institute, Portland, OR) and the German Gene Trap Consortium (GGTC-Partners) for providing us with the REST conditional knockout mice. We are also indebted to dr. Gail Mandel for the kind supply of REST-specific antibodies and to Luigi Naldini (Tiget, Milano, Italy) for lentiviral constructs and protocols. We also thank Drs. Riccardo Navone (Istituto Italiano di

Tecnologia, Genova, Italy), Laura Emionite and Michele Cilli (IRCCS Ospedale Policlinico San Martino, Genova, Italy) for assistance in breeding the mice; drs. Diego Moruzzo and Arta Mehilli (Istituto Italiano di Tecnologia, Genova, Italy) for help in genotyping and cell culture procedures; drs. Ilaria Dallorto and Rossana Ciancio (Istituto Italiano di Tecnologia, Genova, Italy) for administrative assistance. The study was supported by research grants from the Italian Ministry of University and Research (PRIN 2017-A9MK4R and PRIN 2020-WMSNBL to FB), Compagnia di San Paolo, Torino (Grant# 34760 to FB) and IRCCS Ospedale Policlinico San Martino (Ricerca Corrente and “5x1000” to PB, PV and FB).

FUNDING INFORMATION

The authors have no relevant financial or non-financial interests to disclose.

DATA AVAILABILITY STATEMENT

The data that support the findings of this study are available upon request to the corresponding authors.

ORCID

Eleonora Centonze  <https://orcid.org/0000-0003-1802-6471>

Antonella Marte  <https://orcid.org/0000-0001-9842-2663>

Martina Albini  <https://orcid.org/0000-0001-5671-2742>

Anna Rocchi  <https://orcid.org/0000-0002-1334-9063>

Fabrizia Cesca  <https://orcid.org/0000-0003-2190-6314>

Martina Chiacchiaretta  <https://orcid.org/0000-0003-1890-3091>

Thomas Floss  <https://orcid.org/0000-0002-1445-1465>

Pietro Baldelli  <https://orcid.org/0000-0001-9599-3436>

Stefano Ferroni  <https://orcid.org/0000-0001-6211-4220>

Fabio Benfenati  <https://orcid.org/0000-0002-0653-8368>

Pierluigi Valente  <https://orcid.org/0000-0001-6272-1821>

REFERENCES

- Abrahamsen, B., Schneider, N., Erichsen, M. N., Huynh, T. H., Fahlke, C., Bunch, L., & Jensen, A. A. (2013). Allosteric modulation of an excitatory amino acid transporter: The subtype-selective inhibitor UCPH-101 exerts sustained inhibition of EAAT1 through an intramonomeric site in the trimerization domain. *The Journal of Neuroscience*, 33, 1068–1087.
- Abrajano, J. J., Qureshi, I. A., Gokhan, S., Zheng, D., Bergman, A., & Mehler, M. F. (2009a). REST and CoREST modulate neuronal subtype specification, maturation and maintenance. *PLoS One*, 4, e7936.
- Abrajano, J. J., Qureshi, I. A., Gokhan, S., Zheng, D., Bergman, A., & Mehler, M. F. (2009b). Differential deployment of REST and CoREST promotes glial subtype specification and oligodendrocyte lineage maturation. *PLoS One*, 4, e7665.
- Araque, A., Parpura, V., Sanzgiri, R. P., & Haydon, P. G. (1999). Tripartite synapses: Glia, the unacknowledged partner. *Trends in Neurosciences*, 22, 208–215.
- Aronica, E., Ravizza, T., Zurolo, E., & Vezzani, A. (2012). Astrocyte immune responses in epilepsy. *Glia*, 60, 1258–1268.
- Baldelli, P., & Meldolesi, J. (2015). The transcription repressor REST in adult neurons: Physiology, pathology, and diseases. *eNeuro*, 2, ENEURO.0010-15.2015.
- Ballas, N., Grunseich, C., Lu, D. D., Speh, J. C., & Mandel, G. (2005). REST and its corepressors mediate plasticity of neuronal gene chromatin throughout neurogenesis. *Cell*, 121, 645–657.
- Ballas, N., & Mandel, G. (2005). The many faces of REST oversee epigenetic programming of neuronal genes. *Current Opinion in Neurobiology*, 15, 500–506.
- Benfenati, V., Caprini, M., Nobile, M., Rapisarda, C., & Ferroni, S. (2006). Guanosine promotes the upregulation of inward rectifier potassium current mediated by Kir4.1 in cultured rat cortical astrocytes. *Journal of Neurochemistry*, 98, 430–445.
- Bergles, D. E., & Jahr, C. E. (1997). Synaptic activation of glutamate transporters in hippocampal astrocytes. *Neuron*, 19, 1297–1308.
- Bersten, D. C., Wright, J. A., McCarthy, P. J., & Whitelaw, M. L. (2014). Regulation of the neuronal transcription factor NPAS4 by REST and microRNAs. *Biochimica et Biophysica Acta*, 1839, 13–24.
- Bordey, A., & Sontheimer, H. (1997). Postnatal development of ionic currents in rat hippocampal astrocytes in situ. *Journal of Neurophysiology*, 78, 461–477.
- Bruce, A. W., Donaldson, I. J., Wood, I. C., Yerbury, S. A., Sadowski, M. I., Chapman, M., Göttgens, B., & Buckley, N. J. (2004). Genome-wide analysis of repressor element 1 silencing transcription factor/neuron-restrictive silencing factor (REST/NRSF) target genes. *Proceedings of the National Academy of Sciences of the United States of America*, 101, 10458–10463.
- Buono, R. J., Lohoff, F. W., Sander, T., Sperling, M. R., O'Connor, M. J., Dlugos, D. J., Ryan, S. G., Golden, G. T., Zhao, H., Scattergood, T. M., Berrettini, W. H., & Ferraro, T. N. (2004). Association between variation in the human KCNJ10 potassium ion channel gene and seizure susceptibility. *Epilepsy Research*, 58, 175–183.
- Chamberlin, N. L., Traub, R. D., & Dingledine, R. (1990). Role of EPSPs in initiation of spontaneous synchronized burst firing in rat hippocampal neurons bathed in high potassium. *Journal of Neurophysiology*, 64, 1000–1008.
- Chever, O., Djukic, B., McCarthy, K. D., & Amzica, F. (2010). Implication of Kir4.1 channel in excess potassium clearance: An in vivo study on anesthetized glial-conditional Kir4.1 knock-out mice. *The Journal of Neuroscience*, 30, 15769–15777.
- Chiacchiaretta, M., Bramini, M., Rocchi, A., Armirotti, A., Giordano, E., Vázquez, E., Bandiera, T., Ferroni, S., Cesca, F., & Benfenati, F. (2018). Graphene oxide upregulates the homeostatic functions of primary astrocytes and modulates astrocyte-to-neuron communication. *Nano Letters*, 18, 5827–5838.
- Chong, J. A., Tapia-Ramírez, J., Kim, S., Toledo-Aral, J. J., Zheng, Y., Boutros, M. C., Altshuler, Y. M., Frohman, M. A., Kraner, S. D., & Mandel, G. (1995). REST: A mammalian silencer protein that restricts sodium channel gene expression to neurons. *Cell*, 80, 949–957.
- Covey, M. V., Streb, J. W., Spektor, R., & Ballas, N. (2012). REST regulates the pool size of the different neural lineages by restricting the generation of neurons and oligodendrocytes from neural stem/progenitor cells. *Development*, 139, 2878–2890.
- Dallérac, G., Zapata, J., & Rouach, N. (2018). Versatile control of synaptic circuits by astrocytes: Where, when and how? *Nature Reviews Neuroscience*, 19, 729–743.
- D'Ambrosio, R. (2004). The role of glial membrane ion channels in seizures and epileptogenesis. *Pharmacology & Therapeutics*, 103, 95–108.
- D'Ambrosio, R., Maris, D. O., Grady, M. S., Winn, H. R., & Janigro, D. (1999). Impaired K⁺ homeostasis and altered electrophysiological properties of post-traumatic hippocampal glia. *The Journal of Neuroscience*, 19, 8152–8162.
- Danbolt, N. C. (2001). Glutamate uptake. *Progress in Neurobiology*, 65, 1–105.
- De Palma, M., & Naldini, L. (2002). Transduction of a gene expression cassette using advanced generation lentiviral vectors. *Methods in Enzymology*, 346, 514–529.

- Dewald, L. E., Rodriguez, J. P., & Levine, J. M. (2011). The RE1 binding protein REST regulates oligodendrocyte differentiation. *The Journal of Neuroscience*, 31, 3470–3483.
- Djukic, B., Casper, K. B., Philpot, B. D., Chin, L. S., & McCarthy, K. D. (2007). Conditional knock-out of Kir4.1 leads to glial membrane depolarization, inhibition of potassium and glutamate uptake, and enhanced short-term synaptic potentiation. *The Journal of Neuroscience*, 27, 11354–11365.
- Dvorzhak, A., Vagner, T., Kirmse, K., & Grantyn, R. (2016). Functional indicators of glutamate transport in single striatal astrocytes and the influence of Kir4.1 in normal and Huntington mice. *The Journal of Neuroscience*, 36, 4959–4975.
- Ferraro, T. N., Golden, G. T., Smith, G. G., Martin, J. F., Lohoff, F. W., Gieringer, T. A., Zamboni, D., Schwebel, C. L., Press, D. M., Kratzer, S. O., Zhao, H., Berrettini, W. H., & Buono, R. J. (2004). Fine mapping of a seizure susceptibility locus on mouse chromosome 1: Nomination of Kcnj10 as a causative gene. *Mammalian Genome*, 15, 239–251.
- Ferroni, S., Marchini, C., Schubert, P., & Rapisarda, C. (1995). Two distinct inwardly rectifying conductances are expressed in long term dibutylryl-cyclic-AMP treated rat cultured cortical astrocytes. *FEBS Letters*, 367, 319–325.
- Ferroni, S., Valente, P., Caprini, M., Nobile, M., Schubert, P., & Rapisarda, C. (2003). Arachidonic acid activates an open rectifier potassium channel in cultured rat cortical astrocytes. *Journal of Neuroscience Research*, 72, 363–372.
- Gao, Z., Ure, K., Ding, P., Nashaat, M., Yuan, L., Ma, J., Hammer, R. E., & Hsieh, J. (2011). The master negative regulator REST/NRSF controls adult neurogenesis by restraining the neurogenic program in quiescent stem cells. *The Journal of Neuroscience*, 31, 9772–9786.
- Garcia-Manteiga, J. M., D'alessandro, R., & Meldolesi, J. (2020). News about the role of the transcription factor REST in neurons: From physiology to pathology. *International Journal of Molecular Sciences*, 21, 235.
- Grimes, J. A., Nielsen, S. J., Battaglioli, E., Miska, E. A., Speh, J. C., Berry, D. L., Atouf, F., Holdener, B. C., Mandel, G., & Kouzarides, T. (2000). The co-repressor mSin3A is a functional component of the REST-CoREST repressor complex. *The Journal of Biological Chemistry*, 275, 9461–9467.
- Gupta, R. K., & Prasad, S. (2013). Early down regulation of the glial Kir4.1 and GLT-1 expression in pericontusional cortex of the old male mice subjected to traumatic brain injury. *Biogerontology*, 14, 531–541.
- Haydon, P. G. (2001). Glia: Listening and talking to the synapse. *Nature Reviews Neuroscience*, 2, 185–193.
- Hibino, H., Fujita, A., Iwai, K., Yamada, M., & Kurachi, Y. (2004). Differential assembly of inwardly rectifying K⁺ channel subunits, Kir4.1 and Kir5.1, in brain astrocytes. *The Journal of Biological Chemistry*, 279, 44065–33073.
- Hibino, H., Inanobe, A., Furutani, K., Murakami, S., Findlay, I., & Kurachi, Y. (2010). Inwardly rectifying potassium channels: Their structure, function, and physiological roles. *Physiological Reviews*, 90, 291–366.
- Higashi, K., Fujita, A., Inanobe, A., Tanemoto, M., Doi, K., Kubo, T., & Kurachi, Y. (2001). An inwardly rectifying K⁺ channel, Kir4.1, expressed in astrocytes surrounds synapses and blood vessels in brain. *American Journal of Physiology. Cell Physiology*, 281, C922–C931.
- Jaudon, F., Chiacchiarretta, M., Albini, M., Ferroni, S., Benfenati, F., & Cesca, F. (2020). Kidins220/ARMS controls astrocyte calcium signaling and neuron-astrocyte communication. *Cell Death and Differentiation*, 27, 1505–1519.
- Kaesler, P. S., Deng, L., Wang, Y., Dulubova, I., Liu, X., Rizo, J., & Südhof, T. C. (2011). RIM proteins tether Ca²⁺ channels to presynaptic active zones via a direct PDZ-domain interaction. *Cell*, 144, 282–295.
- Kallunki, P., Edelman, G. M., & Jones, F. S. (1998). The neural restrictive silencer element can act as both a repressor and enhancer of L1 cell adhesion molecule gene expression during postnatal development. *Proceedings of the National Academy of Sciences of the United States of America*, 95, 3233–3238.
- Kofuji, P., Ceelen, P., Zahs, K. R., Surbeck, L. W., Lester, H. A., & Newman, E. A. (2000). Genetic inactivation of an inwardly rectifying potassium channel (kir4.1 subunit) in mice: Phenotypic impact in retina. *The Journal of Neuroscience*, 20, 5733–5740.
- Kofuji, P., & Newman, E. A. (2004). Potassium buffering in the central nervous system. *Neuroscience*, 129, 1043–1054.
- Kohyama, J., Sanosaka, T., Tokunaga, A., Takatsuka, E., Tsujimura, K., Okano, H., & Nakashima, K. (2010). BMP-induced REST regulates the establishment and maintenance of astrocytic identity. *The Journal of Cell Biology*, 189, 159–170.
- Kong, Q., Takahashi, K., Schulte, D., Stouffer, N., Lin, Y., & Lin, C. L. (2012). Increased glial glutamate transporter EAAT2 expression reduces epileptogenic processes following pilocarpine-induced status epilepticus. *Neurobiology of Disease*, 47, 145–154.
- Kucheryavykh, Y. V., Kucheryavykh, L. Y., Nichols, C. G., Maldonado, H. M., Baksi, K., Reichenbach, A., Skatchkov, S. N., & Eaton, M. J. (2007). Downregulation of Kir4.1 inward rectifying potassium channel subunits by RNAi impairs potassium transfer and glutamate uptake by cultured cortical astrocytes. *Glia*, 55, 274–281.
- Lee, E. S., Sidoryk, M., Jiang, H., Yin, Z., & Aschner, M. (2009). Estrogen and tamoxifen reverse manganese-induced glutamate transporter impairment in astrocytes. *Journal of Neurochemistry*, 110, 530–544.
- Leis, J. A., Bekar, L. K., & Walz, W. (2005). Potassium homeostasis in the ischemic brain. *Glia*, 50, 407–416.
- Li, L., Head, V., & Timpe, L. C. (2001). Identification of an inward rectifier potassium channel gene expressed in mouse cortical astrocytes. *Glia*, 33, 57–71.
- Liu, Z., Osipovitch, M., Benraiss, A., Huynh, N. P. T., Foti, R., Bates, J., Chandler-Militello, D., Findling, R. L., Tesar, P. J., Nedergaard, M., Windrem, M. S., & Goldman, S. A. (2019). Dysregulated glial differentiation in schizophrenia may be relieved by suppression of SMAD4 and REST-dependent signalling. *Cell Reports*, 27, 3832–3843.
- Murphy-Royal, C., Dupuis, J. P., Varela, J. A., Panatier, A., Pinson, B., Baufreton, J., Groc, L., & Oliet, S. H. (2015). Surface diffusion of astrocytic glutamate transporters shapes synaptic transmission. *Nature Neuroscience*, 18, 219–226.
- Nechiporuk, T., McGann, J., Mullendorff, K., Hsieh, J., Wurst, W., Floss, T., & Mandel, G. (2016). The REST remodeling complex protects genomic integrity during embryonic neurogenesis. *eLife*, 5, e09584.
- Neusch, C., Rozengurt, N., Jacobs, R. E., Lester, H. A., & Kofuji, P. (2001). Kir4.1 potassium channel subunit is crucial for oligodendrocyte development and in vivo myelination. *The Journal of Neuroscience*, 21, 5429–5438.
- Nwaobi, S. E., Cuddapah, V. A., Patterson, K. C., Randolph, A. C., & Olsen, M. L. (2016). The role of glial-specific Kir4.1 in normal and pathological states of the CNS. *Acta Neuropathologica*, 132, 1–21.
- Olsen, M. L., Campbell, S. C., McFerrin, M. B., Floyd, C. L., & Sontheimer, H. (2010). Spinal cord injury causes a wide-spread, persistent loss of Kir4.1 and glutamate transporter 1: Benefit of 17 beta-oestradiol treatment. *Brain*, 133, 1013–1025.
- Olsen, M. L., Campbell, S. L., & Sontheimer, H. (2007). Differential distribution of Kir4.1 in spinal cord astrocytes suggests regional differences in K⁺ homeostasis. *Journal of Neurophysiology*, 98, 786–793.
- Olsen, M. L., Higashimori, H., Campbell, S. L., Hablitz, J. J., & Sontheimer, H. (2006). Functional expression of Kir4.1 channels in spinal cord astrocytes. *Glia*, 53, 516–528.
- Olsen, M. L., Khakh, B. S., Skatchkov, S. N., Zhou, M., Lee, C. J., & Rouach, N. (2015). New insights on astrocyte ion channels: Critical for homeostasis and neuron-glia signaling. *Journal of Neuroscience*, 35, 13827–13835.
- Olsen, M. L., & Sontheimer, H. (2008). Functional implications for Kir4.1 channels in glial biology: From K⁺ buffering to cell differentiation. *Journal of Neurochemistry*, 107, 589–601.

- Pajarillo, E., Demayo, M., Digman, A., Nyarko-Danquah, I., Son, D. S., Aschner, M., & Lee, E. (2022). Deletion of RE1-silencing transcription factor in striatal astrocytes exacerbates manganese-induced neurotoxicity in mice. *Glia*, 70, 1886–1901. <https://doi.org/10.1002/glia.24226>
- Pajarillo, E., Digman, A., Nyarko-Danquah, I., Son, D. S., Soliman, K. F. A., Aschner, M., & Lee, E. (2021). Astrocytic transcription factor REST upregulates glutamate transporter EAAT2, protecting dopaminergic neurons from manganese-induced excitotoxicity. *The Journal of Biological Chemistry*, 297, 101372.
- Pajarillo, E., Rizor, A., Lee, J., Aschner, M., & Lee, E. (2019). The role of astrocytic glutamate transporters GLT-1 and GLAST in neurological disorders: Potential targets for neurotherapeutics. *Neuropharmacology*, 161, 107559.
- Pecoraro Bisogni, F., Lignani, G., Contestabile, A., Castroflorio, E., Pozzi, D., Rocchi, A., Prestigio, C., Orlando, M., Valente, P., Massacesi, M., Benfenati, F., & Baldelli, P. (2018). REST-dependent presynaptic homeostasis induced by chronic neuronal hyperactivity. *Molecular Neurobiology*, 55, 4959–4972.
- Perera, A., Eisen, D., Wagner, M., Laube, S. K., Künzel, A. F., Koch, S., Steinbacher, J., Schulze, E., Splith, V., Mittermeier, N., Müller, M., Biel, M., Carell, T., & Michalakis, S. (2015). TET3 for context-specific hydroxymethylation and induction of gene expression. *Cell Reports*, 11, 283–294.
- Petr, G. T., Sun, Y., Frederick, N. M., Zhou, Y., Dhamne, S. C., Hameed, M. Q., Miranda, C., Bedoya, E. A., Fischer, K. D., Armsen, W., Wang, J., Danbolt, N. C., Rotenberg, A., Aoki, C. J., & Rosenberg, P. A. (2015). Conditional deletion of the glutamate transporter GLT-1 reveals that astrocytic GLT-1 protects against fatal epilepsy while neuronal GLT-1 contributes significantly to glutamate uptake into synaptosomes. *The Journal of Neuroscience*, 35, 5187–5201.
- Pozzi, D., Lignani, G., Ferrea, E., Contestabile, A., Paonessa, F., D'Alessandro, R., Lippiello, P., Boido, D., Fassio, A., Meldolesi, J., Valtorta, F., Benfenati, F., & Baldelli, P. (2013). REST / NRSF-mediated intrinsic homeostasis protects neuronal networks from hyperexcitability. *The EMBO Journal*, 32, 2994–3007.
- Prestigio, C., Ferrante, D., Marte, A., Romei, A., Lignani, G., Onofri, F., Valente, P., Benfenati, F., & Baldelli, P. (2021). REST/NRSF drives homeostatic plasticity of inhibitory synapses in a target-dependent fashion. *eLife*, 10, 1–34.
- Prestigio, C., Ferrante, D., Valente, P., Casagrande, S., Albanesi, E., Yanagawa, Y., Benfenati, F., & Baldelli, P. (2019). Spike-related electrophysiological identification of cultured hippocampal excitatory and inhibitory neurons. *Molecular Neurobiology*, 56, 6276–6292.
- Quesseveur, G., Gardier, A. M., & Guiard, B. P. (2013). The monoaminergic tripartite synapse: A putative target for currently available antidepressant drugs. *Current Drug Targets*, 14, 1277–1294.
- Ransom, B. R., & Goldring, S. (1973). Ionic determinants of membrane potential of cells presumed to be glia in cerebral cortex of cat. *Journal of Neurophysiology*, 36, 855–868.
- Rocchi, A., Carminati, E., De Fusco, A., Kowalska, J. A., Floss, T., & Benfenati, F. (2021). REST/NRSF deficiency impairs autophagy and leads to cellular senescence in neurons. *Aging Cell*, 20, e13471.
- Rothstein, J. D., Dykes-Hoberg, M., Pardo, C. A., Bristol, L. A., Jin, L., Kuncl, R. W., Kanai, Y., Hediger, M. A., Wang, Y., Schielke, J. P., & Welty, D. F. (1996). Knockout of glutamate transporters reveals a major role for astroglial transport in excitotoxicity and clearance of glutamate. *Neuron*, 16, 675–686.
- Rothstein, J. D., Martin, L., Levey, A. I., Dykes-Hoberg, M., Jin, L., Wu, D., Nash, N., & Kuncl, R. W. (1994). Localization of neuronal and glial glutamate transporters. *Neuron*, 13, 713–725.
- Ryoo, K., & Park, J. Y. (2016). Two-pore domain potassium channels in astrocytes. *Experimental Neurobiology*, 25, 222–232.
- Schoenherr, C. J., & Anderson, D. J. (1995). The neuron-restrictive silencer factor (NRSF): A coordinate repressor of multiple neuron-specific genes. *Science*, 267, 1360–1363.
- Schoenherr, C. J., Paquette, A. J., & Anderson, D. J. (1996). Identification of potential target genes for the neuron-restrictive silencer factor. *Proceedings of the National Academy of Sciences of the United States of America*, 93, 9881–9886.
- Schreiner, A. E., Durry, S., Aida, T., Stock, M. C., Rütger, U., Tanaka, K., Rose, C. R., & Kafitz, K. W. (2014). Laminar and subcellular heterogeneity of GLAST and GLT-1 immunoreactivity in the developing postnatal mouse hippocampus. *The Journal of Comparative Neurology*, 522, 204–224.
- Seifert, G., Hüttmann, K., Binder, D. K., Hartmann, C., Wyczynski, A., Neusch, C., & Steinhäuser, C. (2009). Analysis of astroglial K⁺ channel expression in the developing hippocampus reveals a predominant role of the Kir4.1 subunit. *The Journal of Neuroscience*, 29, 7474–7488.
- Shimamoto, K., Lebrun, B., Yasuda-Kamatani, Y., Sakaitani, M., Shigeri, Y., Yumoto, N., & Nakajima, T. (1998). DL-threo-beta-benzoyloxyaspartate, a potent blocker of excitatory amino acid transporters. *Molecular Pharmacology*, 53, 195–201.
- Stevens, C. F. (1993). Quantal release of neurotransmitter and long-term potentiation. *Cell*, 72, 55–63.
- Sulkowski, G., Dabrowska-Bouta, B., Salinska, E., & Struzynska, L. (2014). Modulation of glutamate transport and receptor binding by glutamate receptor antagonists in EAE rat brain. *PLoS One*, 9, e113954.
- Theodosios, D. T., Poulain, D. A., & Oliet, S. H. (2008). Activity-dependent structural and functional plasticity of astrocyte-neuron interactions. *Physiological Reviews*, 88, 983–1008.
- Tureček, R., & Trussell, L. O. (2000). Control of synaptic depression by glutamate transporters. *The Journal of Neuroscience*, 20, 2054–2063.
- Tzingounis, A. V., & Wadiche, J. I. (2007). Glutamate transporters: Confining runaway excitation by shaping synaptic transmission. *Nature Reviews. Neuroscience*, 8, 935–947.
- Valente, P., Lignani, G., Medrihan, L., Bosco, F., Contestabile, A., Lippiello, P., Ferrea, E., Schachner, M., Benfenati, F., Giovedi, S., & Baldelli, P. (2016). Cell adhesion molecule L1 contributes to neuronal excitability regulating the function of voltage-gated Na⁺ channels. *Journal of Cell Science*, 129, 1878–1891.
- Verkhratsky, A., & Nedergaard, M. (2018). Physiology of astroglia. *Physiological Reviews*, 98, 239–389.
- Verkhratsky, A., & Steinhäuser, C. (2000). Ion channels in glial cells. *Brain Research Reviews*, 32, 380–412.
- Vezzani, A., Maroso, M., Balosso, S., Sanchez, M. A., & Bartfai, T. (2011). IL-1 receptor/toll-like receptor signaling in infection, inflammation, stress and neurodegeneration couples hyperexcitability and seizures. *Brain, Behavior, and Immunity*, 25, 1281–1289.
- Walz, W. (2000). Role of astrocytes in the clearance of excess extracellular potassium. *Neurochemistry International*, 36, 291–300.
- Watt, A. J., Van Rossum, M. C. W., MacLeod, K. M., Nelson, S. B., & Turrigiano, G. G. (2000). Activity coregulates quantal AMPA and NMDA currents at neocortical synapses. *Neuron*, 26, 659–670.
- Zhao, Y., Zhu, M., Yu, Y., Qiu, L., Zhang, Y., & Zhang, J. (2017). Brain REST/NRSF is not only a silent repressor but also an active protector. *Molecular Neurobiology*, 54, 541–550.
- Zheng, D., Zhao, K., & Mehler, M. F. (2009). Profiling RE1/REST-mediated histone modifications in the human genome. *Genome Biology*, 10, R9.
- Zhou, M., Xu, G., Xie, M., Zhang, X., Schools, G. P., Ma, L., Kimelberg, H. K., & Chen, H. (2009). TWIK-1 and TREK-1 are potassium channels contributing significantly to astrocyte passive conductance in rat hippocampal slices. *The Journal of Neuroscience*, 29, 8551–8564.

Zurolo, E., de Groot, M., Iyer, A., Anink, J., van Vliet, E. A., Heimans, J. J., Reijneveld, J. C., Gorter, J. A., & Aronica, E. (2012). Regulation of Kir4.1 expression in astrocytes and astrocytic tumors: A role for interleukin-1 β . *Journal of Neuroinflammation*, 9, 280.